

N 69 29725

NASA TECHNICAL
MEMORANDUM

NASA TMX 53838

Report No. 53838

THE MOLECULAR KINETICS OF THE BAYARD-ALPERT AND
MODIFIED REDHEAT VACUUM GAUGES USED ON
EXPLORER XVII AND EXPLORER XXXII

By James O. Ballance
Aero-Astrodynamic Laboratory

April 28, 1969

CASE FILE
COPY

NASA

*George C. Marshall Space Flight Center
Marshall Space Flight Center, Alabama*

TECHNICAL REPORT STANDARD TITLE PAGE

1. Report No. NASA TM X-53838	2. Government Accession No.	3. Recipient's Catalog No.	
4. Title and Subtitle THE MOLECULAR KINETICS OF THE BAYARD-ALPERT AND MODIFIED REDHEAT VACUUM GAUGES USED ON EXPLORER XVII AND EXPLORER XXXII		5. Report Date April 28, 1969	
7. Author(s) James O. Ballance		6. Performing Organization Code	
9. Performing Organization Name and Address Aero-Astrodynamic Laboratory Fluid Mechanics Research Office Marshall Space Flight Center, Alabama 35812		8. Performing Organization Report No.	
12. Sponsoring Agency Name and Address Same as 9		10. Work Unit No.	
		11. Contract or Grant No.	
		13. Type of Report and Period Covered NASA Technical Memorandum	
		14. Sponsoring Agency Code	
15. Supplementary Notes			
16. Abstract A Monte Carlo computer analysis of the internal free-molecular-flow characteristics of the modified Redhead Magnetron and the Bayard-Alpert vacuum gauges used on Explorer XVII and Explorer XXXII satellites has been conducted. Although the transmission probabilities for the gauges were determined for a simplified geometric configuration, the results should be valid since a similar approach to the mass spectrometer gauge of the thermosphere probe used on sounding rockets yielded very valid results. The effects of specular reflections from the walls were examined, and a simple time response model of the gauges was determined.			
17. Key Words		18. Distribution Statement Public Release	
19. Security Classif. (of this report) U	20. Security Classif. (of this page) U	21. No. of Pages 62	22. Price

DEFINITION OF SYMBOLS

<u>Symbol</u>	<u>Definition</u>
$F(S)$	$e^{-S^2} + \sqrt{\pi} S [1 + ERF(S)]$
A	radius
k	Boltzmann's constant
m	mass of molecule
\bar{v}	average speed of molecule
v_m	most probable speed of molecule
N	number density of molecules
T	absolute temperature
U	free stream velocity
α	angle of attack
S	speed ratio, $U \cos \alpha / v_m$
L	length of duct
$K(G, S, \alpha)$	Clausing probability factor (transmission probability)
Z	number of molecules
P	pressure
A_o	area of entrance orifice
A_i	area of exit orifice

TECHNICAL MEMORANDUM X-53838

THE MOLECULAR KINETICS OF THE BAYARD-ALPERT AND
MODIFIED REDHEAT VACUUM GAUGES USED ON
EXPLORER XVII AND EXPLORER XXXII

SUMMARY

A Monte Carlo computer analysis of the internal free-molecular-flow characteristics of the modified Redhead Magnetron and the Bayard-Alpert vacuum gauges used on Explorer XVII and Explorer XXXII satellites has been conducted. Although the transmission probabilities for the gauges were determined for a simplified geometric configuration, the results should be valid since a similar approach to the mass spectrometer gauge of the thermosphere probe used on sounding rockets yielded very valid results. The effects of specular reflections from the walls were examined, and a simple time response model of the gauges was determined.

I. INTRODUCTION

The Explorer XVII and Explorer XXXII satellites were designed to measure in situ the neutral particle density, composition, temperature, and the electron density and temperature in the upper atmosphere. Among the sensors on these satellites were Bayard-Alpert and Modified Redhead Magnetron Vacuum Gauges. These satellites, their gauges, and results are described in References 1 through 8.

The neutral-particle density determined from the measurements of these gauges differed greatly from the density as determined from the drag on the satellite. Several reasons for this difference have been suggested. The original analysis of the response of these gauges considered the flow to be through an ideal orifice with the instrument cavity representing the volume behind the orifice. This same approach to the thermosphere-probe response led to a difference of nearly 20 percent between the theoretical and measured values. Since a Monte Carlo analysis of the thermosphere probe greatly improved the analysis of the data, it was felt that a similar analysis of the satellite gauges might also improve their analysis. Furthermore, it was hoped that the gauge response characteristic might yield some useful information on the gas molecule-surface interactions which occur at orbital velocities. This report describes the Monte Carlo analysis of the system, and presents the results of the analysis.

II. GEOMETRICAL CONFIGURATIONS USED FOR THE ANALYSIS

A. Modified Redhead Gauge

The modified Redhead gauges used on the Explorer XVII and XXXII satellites were basically a cylindrical tube with an ID of 1 1/6 inches and a length of 5 3/8 inches (see figure 33a). An entrance orifice of 3/8-inch diameter was connected to the inner diameter by a short conical section. The electrodes were 7/8-inch in diameter with the first electrode approximately 3 3/4 inches from the orifice and the distance between the electrodes about 3/4 inch. It is in the volume between the electrodes where the discharge takes place and the ions counted. Following the thermosphere analysis, this geometry was simplified by eliminating the short conical section of the tube; therefore, all molecules entering the orifice, traversing the tube, and passing in the annular region between the walls of the tube and the first electrode were considered to have reached the sensing volume.

B. Bayard-Alpert Gauge

The Bayard-Alpert gauges were cylindrical tubes, 5 3/8 inches long, with a one-inch ID and a 3/8-inch diameter orifice connected to the inner diameter by a short conical section (see figure 33b). The sensing volume in this gauge is within the coaxial collector grid which begins about 3 3/8 inches from the orifice. Thus, molecules entering the orifice, traversing the tube and crossing an imaginary plane at the end of the grid structure were considered to have entered the sensing volume. Again the short conical section of the tube was eliminated for the computer analysis.

C. Limitations Due to Modified Geometry

In the thermosphere probe analysis, it was noted that the calculated transmission probabilities and subsequent response calculations did not agree well with the flight data at very high angles of attack. This is most likely due to the elimination of the short conical section within the gauge for ease of computation. For the satellite speeds, this feature should cause even a larger error than that with the sounding rocket probe.

III. COMPUTER RESULTS

A. General Remarks

A Monte Carlo analysis of the two configurations considered was made for angles of attack of 0° , 5° , 10° , 15° , 20° , 25° , 30° , 45° , 60° , 75° , and 90° . Speed ratios of 2, 3, 4, 5, 6, 7, 8, and 9 were considered with an additional speed ratio of 7.5 for the Bayard-Alpert gauge. Each molecule was followed until it exited the tube (either back through the orifice or into the sensing volume) or until it made 350 collisions. Very few molecules (i.e., ≈ 0.05 percent) underwent that many collisions before exiting.

The transmission probability, K, (the probability that a molecule entering the orifice will pass through the tube and enter the sensor volume) is required to relate the density measured in the sensor volume to the ambient density through which the probe is passing. The equations for this relationship involving the transmission probability are shown in Appendix A. K is a function of the geometry, the speed ratio, the angle of attack, and the type of reflection a molecule makes after colliding with the surface. For vacuum systems where the mass velocity of the gas is small in comparison with the mean thermal speed of the molecules, diffuse reflections are assumed. As the mass velocity increases, as in a rocket probe, this may not be true. Accordingly, a program was written so that the molecules could make some number of specular collisions, and, after that number, the remaining collisions, until they exited, were diffuse. The notation used to identify this parameter is as follows: zero specular, meaning all reflections are diffuse; 1 specular, meaning that the first collision was specular and all subsequent diffuse; 2 specular, meaning that the first two collisions were specular and all subsequent diffuse, etc. The results of changing the parameter are clearly identified. It is not intended to suggest that the above model is correct. It was used only to examine the influence of such a model on the response of the probe.

In addition to transmission probability, some information can be obtained from the program concerning the time of passage from the orifice to the sensor. This was done by assuming that the molecules traveled at the relative mass velocity of the probe until they were diffusely reflected from the walls, at which time they traveled at a speed representative of the temperature of the probe. While these results are certainly not exact, they should point out any major time response problem if one existed.

B. Transmission Probabilities for the Redhead Gauge

Tables 1 through 7 present the transmission probabilities for the modified Redhead gauge at various angles of attack. Also presented on each table is the transmission probability with no mass motion and the ratio $K(G,S,\alpha)/K(G,0,0)$ required for relating the measured pressure to the ambient pressure as shown in Appendix A. Figures 1 through 7 show these same transmission probabilities graphically and indicate the general trend of the values rather than exact graphical representations.

The general trend of the data seems to be quite consistent with the physical system. For the completely diffuse reflection case, the transmission probability generally increases with increasing speed ratio. For specular reflection, the transmission probability decreases with increasing speed ratio at zero angle of attack, but increases at the same angle of attack. Physically, the data show that when the speed ratio is large and the angle of attack low, most of the molecules entering the orifice traverse the tube and hit the first electrode. Those having a diffuse reflection are redistributed along the tube walls more uniformly than those which are specularly reflected back toward the orifice where their probability of exiting back to ambient conditions is much higher. Figures 8 through 14 show the theoretical pressure ratio response, $(P_s/P_o)(T_o/T_s)^{1/2}$, as a function of the angle of attack.

C. Transmission Probabilities for the Bayard-Alpert Gauge

Tables 8 through 16 present the transmission probabilities for the Bayard-Alpert gauge at various angles of attack. Again, the transmission probability for no mass motion is also presented and the ratio $K(G,S,\alpha)/K(G,0,0)$. Figures 15 through 23 present the same data graphically. For this gauge, the number of specular reflections does not influence the response of the gauge as strongly as with the modified Redhead gauge. This is due to the "open" geometry into the sensor volume where counting takes place.

Figures 24 through 31 show the theoretical pressure ratio response, $(P_s/P_o)(T_o/T_s)^{1/2}$, as a function of the angle of attack.

D. Time Response

Figure 32, which presents the typical time response data which were determined in the analysis, shows the time required for the total number of particles to reach the sensor volume. Explorer XVII had a spin period

of about .67 second and Explorer XXXII about two seconds. When the minimum angle of attack during a tumble cycle was 0° for Explorer XVII, it would take about 1.9 milliseconds to sweep an angle of 1° . Figure 32 shows that it requires about 140 milliseconds for the total number to reach the sensor volume. Thus, the group of molecules entering the gauge when the angle of attack is zero will not be completely counted until the satellite has spun through an angle of nearly 75 degrees. For Explorer XXXII, the angle is less, about 25 degrees. In either case, this time delay could be a major problem in analysis of the data.

IV. DISCUSSION

The analysis of the molecular kinetics within the modified Redhead gauge and the Bayard-Alpert gauge reveals that the initial gas-surface-interaction model greatly influences the response of the gauge. While the transmission probabilities vary greatly with angle of attack for all speed ratios, the pressure ratio response function, $(P_s/P_0)(T_0/T_s)^{1/2}$, is significantly affected only at the higher speed ratios, i.e., $S > 5$. This effect is manifested more in the modified Redhead gauge than in the Bayard-Alpert gauge due, most likely, to the more complex geometry of the former gauge. Since the speed ratio for the satellites is usually greater than 5, flight data in the Redhead gauge might indicate which gas-surface interaction model most nearly predicts the actual response. However, the time response characteristics of the gauges coupled with the spin rate of the satellite may lead to an integrating type of response which will mask the theoretically predicted structure. A preliminary study indicated that this was the case, and a more exhaustive analysis is in process.

TABLE 1

TRANSMISSION PROBABILITIES FOR THE VACUUM
GAUGES ON THE EXPLORER XVII AND EXPLORER XXXII
AERONOMY SATELLITES

SPEED RATIO = 2.0 $K(G,0,0) = .523$
REDHEAD GAUGE

NO SPECULAR REFLECTIONS

ANGLE OF ATTACK	$K(G,S,A)$	$K(G,S,A)/K(G,0,0)$
0	.5710	1.0918
5	.5624	1.0753
10	.5538	1.0589
15	.5518	1.0551
20	.5439	1.0400
25	.5383	1.0293
30	.5311	1.0155
45	.5152	,9851
60	.5037	,9631
75	.4831	,9237
90	.5022	,9602

ONE SPECULAR REFLECTION

ANGLE OF ATTACK	$K(G,S,A)$	$K(G,S,A)/K(G,0,0)$
0	.6400	1.2237
5	.6273	1.1994
10	.6290	1.2027
15	.6336	1.2115
20	.6164	1.1786
25	.6072	1.1610
30	.6058	1.1583
45	.5691	1.0881
60	.5520	1.0554
75	.5305	1.0143
90	.5172	,9889

TWO SPECULAR REFLECTIONS

ANGLE OF ATTACK	$K(G,S,A)$	$K(G,S,A)/K(G,0,0)$
0	.6215	1.1883
5	.6141	1.1742
10	.6275	1.1998
15	.6232	1.1916
20	.6223	1.1899
25	.6288	1.2023
30	.6257	1.1964
45	.6061	1.1589
60	.5936	1.1350
75	.5698	1.0895
90	.5506	1.0528

TABLE 2

TRANSMISSION PROBABILITIES FOR THE VACUUM
GAUGES ON THE EXPLORER XVII AND EXPLORER XXXII
AERONOMY SATELLITES

SPEED RATIO = 3.0 $K(G,0,0) = .523$

REDHEAD GAUGE

NO SPECULAR REFLECTIONS

ANGLE OF ATTACK	$K(G,S,A)$	$K(G,S,A)/K(G,0,0)$
0	.6056	1.1579
5	.5923	1.1325
10	.5830	1.1147
15	.5670	1.0841
20	.5507	1.0530
25	.5345	1.0220
30	.5392	1.0310
45	.5018	.9595
60	.5098	.9748
75	.4936	.9438
90	.4969	.9501

ONE SPECULAR REFLECTION

ANGLE OF ATTACK	$K(G,S,A)$	$K(G,S,A)/K(G,0,0)$
0	.6533	1.2491
5	.6545	1.2514
10	.6651	1.2717
15	.6552	1.2528
20	.6319	1.2082
25	.6317	1.2078
30	.6126	1.1713
45	.5687	1.0874
60	.5358	1.0245
75	.5187	.9918
90	.5117	.9784

TWO SPECULAR REFLECTIONS

ANGLE OF ATTACK	$K(G,S,A)$	$K(G,S,A)/K(G,0,0)$
0	.6131	1.1723
5	.6229	1.1910
10	.6265	1.1979
15	.6309	1.2063
20	.6411	1.2258
25	.6371	1.2182
30	.6389	1.2216
45	.6176	1.1809
60	.5652	1.0807
75	.5410	1.0344
90	.5219	.9979

TABLE 3

TRANSMISSION PROBABILITIES FOR THE VACUUM
GAUGES ON THE EXPLORER XVII AND EXPLORER XXXII
AERONOMY SATELLITES

SPEED RATIO = 4.0 $K(G,0,0) = .523$
REDHEAD GAUGE

NO SPECULAR REFLECTIONS

ANGLE OF ATTACK	$K(G,S,A)$	$K(G,S,A)/K(G,0,0)$
0	.6337	1.2117
5	.6157	1.1772
10	.6116	1.1694
15	.5864	1.1212
20	.5577	1.0663
25	.5418	1.0359
30	.5370	1.0268
45	.4995	.9551
60	.5065	.9685
75	.4916	.9400
90	.4983	.9528

ONE SPECULAR REFLECTION

ANGLE OF ATTACK	$K(G,S,A)$	$K(G,S,A)/K(G,0,0)$
0	.6571	1.2564
5	.6597	1.2614
10	.6706	1.2822
15	.6679	1.2771
20	.6521	1.2468
25	.6375	1.2189
30	.6322	1.2088
45	.5674	1.0849
60	.5368	1.0264
75	.5049	.9654
90	.4980	.9522

TWO SPECULAR REFLECTIONS

ANGLE OF ATTACK	$K(G,S,A)$	$K(G,S,A)/K(G,0,0)$
0	.6043	1.1554
5	.6054	1.1576
10	.6185	1.1826
15	.6278	1.2004
20	.6428	1.2291
25	.6665	1.2744
30	.6595	1.2610
45	.6232	1.1916
60	.5713	1.0924
75	.5266	1.0069
90	.5107	.9765

TABLE 4.

TRANSMISSION PROBABILITIES FOR THE VACUUM
GAUGES ON THE EXPLORER XVII AND EXPLORER XXXII
AERONOMY SATELLITES

SPEED RATIO = 5.0 $K(G,0,0) = .523$
REDHEAD GAUGE

NO SPECULAR REFLECTIONS

ANGLE OF ATTACK	$K(G,S,A)$	$K(G,S,A)/K(G,0,0)$
0	.6449	1.2331
5	.6339	1.2120
10	.6226	1.1904
15	.5944	1.1365
20	.5580	1.0669
25	.5441	1.0403
30	.5324	1.0180
45	.5006	.9572
60	.5143	.9834
75	.4937	.9440
90	.4917	.9402

ONE SPECULAR REFLECTION

ANGLE OF ATTACK	$K(G,S,A)$	$K(G,S,A)/K(G,0,0)$
0	.6497	1.2423
5	.6613	1.2644
10	.6754	1.2914
15	.6677	1.2767
20	.6597	1.2614
25	.6549	1.2522
30	.6301	1.2048
45	.5613	1.0732
60	.5303	1.0140
75	.4990	.9541
90	.5020	.9598

TWO SPECULAR REFLECTIONS

ANGLE OF ATTACK	$K(G,S,A)$	$K(G,S,A)/K(G,0,0)$
0	.5873	1.1229
5	.5809	1.1107
10	.6113	1.1688
15	.6213	1.1880
20	.6522	1.2470
25	.6735	1.2878
30	.6769	1.2943
45	.6192	1.1839
60	.5559	1.0629
75	.5258	1.0054
90	.5060	.9675

TABLE 5

 TRANSMISSION PROBABILITIES FOR THE VACUUM
 GAUGES ON THE EXPLORER XVII AND EXPLORER XXXII
 AERONOMY SATELLITES

 SPEED RATIO = 6.0 $K(G,0,0) = .523$
 REDHEAD GAUGE

NO SPECULAR REFLECTIONS

ANGLE OF ATTACK	$K(G,S,A)$	$K(G,S,A)/K(G,0,0)$
0	.6605	1.2629
5	.6535	1.2495
10	.6281	1.2010
15	.5917	1.1314
20	.5560	1.0631
25	.5397	1.0319
30	.5319	1.0170
45	.5037	.9631
60	.5014	.9587
75	.4921	.9409
90	.5081	.9715

ONE SPECULAR REFLECTION

ANGLE OF ATTACK	$K(G,S,A)$	$K(G,S,A)/K(G,0,0)$
0	.6398	1.2233
5	.6558	1.2539
10	.6709	1.2828
15	.6750	1.2906
20	.6695	1.2801
25	.6542	1.2509
30	.6374	1.2187
45	.5636	1.0776
60	.5318	1.0168
75	.5023	.9604
90	.5003	.9566

TWO SPECULAR REFLECTIONS

ANGLE OF ATTACK	$K(G,S,A)$	$K(G,S,A)/K(G,0,0)$
0	.5749	1.0992
5	.5717	1.0931
10	.5971	1.1417
15	.6165	1.1788
20	.6487	1.2403
25	.6681	1.2774
30	.6867	1.3130
45	.6242	1.1935
60	.5582	1.0673
75	.5134	.9816
90	.4917	.9402

TABLE 6

TRANSMISSION PROBABILITIES FOR THE VACUUM
GAUGES ON THE EXPLORER XVII AND EXPLORER XXXII
AERONOMY SATELLITES

SPEED RATIO = 7.0 $K(G,0,0) = .523$
REDHEAD GAUGE

NO SPECULAR REFLECTIONS

ANGLE OF ATTACK	$K(G,S,A)$	$K(G,S,A)/K(G,0,0)$
0	.6708	1.2826
5	.6603	1.2625
10	.6494	1.2417
15	.5898	1.1277
20	.5613	1.0732
25	.5363	1.0254
30	.5263	1.0063
45	.5040	.9637
60	.4999	.9558
75	.4957	.9478
90	.5019	.9597

ONE SPECULAR REFLECTION

ANGLE OF ATTACK	$K(G,S,A)$	$K(G,S,A)/K(G,0,0)$
0	.6354	1.2149
5	.6573	1.2568
10	.6895	1.3184
15	.6789	1.2981
20	.6739	1.2885
25	.6642	1.2700
30	.6291	1.2029
45	.5584	1.0677
60	.5499	1.0514
75	.4962	.9488
90	.5019	.9597

TWO SPECULAR REFLECTIONS

ANGLE OF ATTACK	$K(G,S,A)$	$K(G,S,A)/K(G,0,0)$
0	.5585	1.0679
5	.5713	1.0924
10	.5841	1.1168
15	.6204	1.1862
20	.6498	1.2424
25	.6839	1.3076
30	.6812	1.3025
45	.6333	1.2109
60	.5657	1.0816
75	.5088	.9728
90	.4876	.9323

TABLE 7

TRANSMISSION PROBABILITIES FOR THE VACUUM
GAUGES ON THE EXPLORER XVII AND EXPLORER XXXII
AERONOMY SATELLITES

SPEED RATIO = 8.0 $K(G,0,0) = .523$
REDHEAD GAUGE

NO SPECULAR REFLECTIONS

ANGLE OF ATTACK	$K(G,S,A)$	$K(G,S,A)/K(G,0,0)$
0	.6682	1.2776
5	.6692	1.2795
10	.6398	1.2233
15	.5904	1.1289
20	.5601	1.0709
25	.5281	1.0098
30	.5309	1.0151
45	.4989	.9539
60	.5058	.9671
75	.4930	.9426
90	.5069	.9692

ONE SPECULAR REFLECTION

ANGLE OF ATTACK	$K(G,S,A)$	$K(G,S,A)/K(G,0,0)$
0	.6129	1.1719
5	.6465	1.2361
10	.6853	1.3103
15	.6756	1.2918
20	.6738	1.2883
25	.6731	1.2870
30	.6345	1.2132
45	.5637	1.0778
60	.5323	1.0178
75	.5022	.9602
90	.5021	.9600

TWO SPECULAR REFLECTIONS

ANGLE OF ATTACK	$K(G,S,A)$	$K(G,S,A)/K(G,0,0)$
0	.5661	1.0824
5	.5656	1.0815
10	.5801	1.1092
15	.6049	1.1566
20	.6574	1.2570
25	.6931	1.3252
30	.6844	1.3086
45	.6375	1.2189
60	.5853	1.1191
75	.5084	.9721
90	.4974	.9511

TABLE 8

TRANSMISSION PROBABILITIES FOR THE VACUUM
GAUGES ON THE EXPLORER XVII AND EXPLORER XXXII
AERONOMY SATELLITES

SPEED RATIO = 2.0 $K(G,0,0) = .686$

BAYARD-ALPERT GAUGE

NO SPECULAR REFLECTIONS

ANGLE OF ATTACK	$K(G,S,A)$	$K(G,S,A)/K(G,0,0)$
0	.7510	1.0948
5	.7510	1.0948
10	.7490	1.0918
15	.7350	1.0714
20	.7270	1.0598
25	.7280	1.0612
30	.7010	1.0219
45	.6800	.9913
60	.6690	.9752
75	.6660	.9708
90	.6560	.9563

ONE SPECULAR REFLECTION

ANGLE OF ATTACK	$K(G,S,A)$	$K(G,S,A)/K(G,0,0)$
0	.8570	1.2493
5	.8610	1.2551
10	.8550	1.2464
15	.8490	1.2376
20	.8370	1.2201
25	.8240	1.2012
30	.8100	1.1808
45	.7650	1.1152
60	.7430	1.0831
75	.7140	1.0408
90	.6910	1.0073

TWO SPECULAR REFLECTIONS

ANGLE OF ATTACK	$K(G,S,A)$	$K(G,S,A)/K(G,0,0)$
0	.8830	1.2872
5	.8801	1.2829
10	.8811	1.2844
15	.8770	1.2784
20	.8690	1.2668
25	.8620	1.2566
30	.8560	1.2478
45	.8160	1.1895
60	.7760	1.1312
75	.7530	1.0977
90	.7370	1.0743

TABLE 9

TRANSMISSION PROBABILITIES FOR THE VACUUM
GAUGES ON THE EXPLORER XVII AND EXPLORER XXXII
AERONOMY SATELLITES

SPEED RATIO = 3.0 $K(G,0,0) = .686$
BAYARD-ALPERT GAUGE

NO SPECULAR REFLECTIONS

ANGLE OF ATTACK	$K(G,S,A)$	$K(G,S,A)/K(G,0,0)$
0	.7980	1.1633
5	.7920	1.1545
10	.7750	1.1297
15	.7570	1.1035
20	.7420	1.0816
25	.7250	1.0569
30	.7090	1.0335
45	.6770	,9869
60	.6630	,9665
75	.6530	,9519
90	.6650	,9694

ONE SPECULAR REFLECTION

ANGLE OF ATTACK	$K(G,S,A)$	$K(G,S,A)/K(G,0,0)$
0	.8950	1.3047
5	.8970	1.3076
10	.8940	1.3032
15	.8800	1.2828
20	.8670	1.2638
25	.8470	1.2347
30	.8300	1.2099
45	.7570	1.1035
60	.7200	1.0496
75	.6850	,9985
90	.6750	,9840

TWO SPECULAR REFLECTIONS

ANGLE OF ATTACK	$K(G,S,A)$	$K(G,S,A)/K(G,0,0)$
0	.9050	1.3192
5	.9120	1.3294
10	.9080	1.3236
15	.9040	1.3178
20	.8950	1.3047
25	.8900	1.2974
30	.8840	1.2886
45	.8220	1.1983
60	.7660	1.1166
75	.7260	1.0583
90	.7030	1.0248

TABLE 10

TRANSMISSION PROBABILITIES FOR THE VACUUM
GAUGES ON THE EXPLORER XVII AND EXPLORER XXXII
AERONOMY SATELLITES

SPEED RATIO = 4.0 $K(G,0,0) = .686$
BAYARD-ALPERT GAUGE

NO SPECULAR REFLECTIONS

ANGLE OF ATTACK	$K(G,S,A)$	$K(G,S,A)/K(G,0,0)$
0	.8340	1.2157
5	.8210	1.1968
10	.8040	1.1720
15	.7780	1.1341
20	.7440	1.0845
25	.7170	1.0452
30	.7050	1.0277
45	.6660	.9708
60	.6620	.9650
75	.6580	.9592
90	.6710	.9781

ONE SPECULAR REFLECTION

ANGLE OF ATTACK	$K(G,S,A)$	$K(G,S,A)/K(G,0,0)$
0	.9120	1.3294
5	.9210	1.3426
10	.9180	1.3382
15	.8980	1.3090
20	.8860	1.2915
25	.8640	1.2595
30	.8360	1.2187
45	.7540	1.0991
60	.7020	1.0233
75	.6790	.9898
90	.6640	.9679

TWO SPECULAR REFLECTIONS

ANGLE OF ATTACK	$K(G,S,A)$	$K(G,S,A)/K(G,0,0)$
0	.9140	1.3324
5	.9130	1.3309
10	.9120	1.3294
15	.9090	1.3251
20	.9140	1.3324
25	.9070	1.3222
30	.9010	1.3134
45	.8320	1.2128
60	.7600	1.1079
75	.7030	1.0248
90	.6740	.9825

TABLE 11

TRANSMISSION PROBABILITIES FOR THE VACUUM
GAUGES ON THE EXPLORER XVII AND EXPLORER XXXII
AERONOMY SATELLITES

SPEED RATIO = 5.0 $K(G,0,0) = .686$
BAYARD-ALPERT GAUGE

NO SPECULAR REFLECTIONS

ANGLE OF ATTACK	$K(G,S,A)$	$K(G,S,A)/K(G,0,0)$
0	.8690	1.2668
5	.8580	1.2507
10	.8220	1.1983
15	.7820	1.1399
20	.7400	1.0787
25	.7150	1.0423
30	.7060	1.0292
45	.6700	.9767
60	.6690	.9752
75	.6560	.9563
90	.6680	.9738

ONE SPECULAR REFLECTION

ANGLE OF ATTACK	$K(G,S,A)$	$K(G,S,A)/K(G,0,0)$
0	.9140	1.3324
5	.9240	1.3469
10	.9230	1.3455
15	.9120	1.3294
20	.8950	1.3047
25	.8710	1.2697
30	.8460	1.2332
45	.7570	1.1035
60	.7030	1.0248
75	.6720	.9796
90	.6540	.9534

TWO SPECULAR REFLECTIONS

ANGLE OF ATTACK	$K(G,S,A)$	$K(G,S,A)/K(G,0,0)$
0	.9160	1.3353
5	.9150	1.3338
10	.9080	1.3236
15	.9100	1.3265
20	.9180	1.3382
25	.9140	1.3324
30	.9070	1.3222
45	.8360	1.2187
60	.7580	1.1050
75	.6960	1.0146
90	.6650	.9694

TABLE 12

TRANSMISSION PROBABILITIES FOR THE VACUUM
GAUGES ON THE EXPLORER XVII AND EXPLORER XXXII
AERONOMY SATELLITES

SPEED RATIO = 6.0 $K(G,0,0) = .686$
BAYARD-ALPERT GAUGE

NO SPECULAR REFLECTIONS

ANGLE OF ATTACK	$K(G,S,A)$	$K(G,S,A)/K(G,0,0)$
0	.8860	1.2915
5	.8770	1.2784
10	.8410	1.2259
15	.7920	1.1545
20	.7430	1.0831
25	.7140	1.0408
30	.7010	1.0219
45	.6630	.9665
60	.6620	.9650
75	.6550	.9548
90	.6690	.9752

ONE SPECULAR REFLECTION

ANGLE OF ATTACK	$K(G,S,A)$	$K(G,S,A)/K(G,0,0)$
0	.9100	1.3265
5	.9240	1.3469
10	.9230	1.3455
15	.9190	1.3397
20	.9110	1.3280
25	.8810	1.2843
30	.8460	1.2332
45	.7480	1.0904
60	.7130	1.0394
75	.6640	.9679
90	.6520	.9504

TWO SPECULAR REFLECTIONS

ANGLE OF ATTACK	$K(G,S,A)$	$K(G,S,A)/K(G,0,0)$
0	.9200	1.3411
5	.9130	1.3309
10	.9110	1.3280
15	.8990	1.3105
20	.9180	1.3382
25	.9250	1.3484
30	.9210	1.3426
45	.8400	1.2245
60	.7450	1.0860
75	.6850	.9985
90	.6710	.9781

TABLE 13

TRANSMISSION PROBABILITIES FOR THE VACUUM
GAUGES ON THE EXPLORER XVII AND EXPLORER XXXII
AERONOMY SATELLITES

SPEED RATIO = 7.0 $K(G,0,0) = .686$
BAYARD-ALPERT GAUGE

NO SPECULAR REFLECTIONS

ANGLE OF ATTACK	$K(G,S,A)$	$K(G,S,A)/K(G,0,0)$
0	.9120	1.3294
5	.8850	1.2901
10	.8490	1.2376
15	.7920	1.1545
20	.7400	1.0787
25	.7110	1.0364
30	.6940	1.0117
45	.6630	.9665
60	.6640	.9679
75	.6760	.9854
90	.6670	.9723

ONE SPECULAR REFLECTION

ANGLE OF ATTACK	$K(G,S,A)$	$K(G,S,A)/K(G,0,0)$
0	.9070	1.3222
5	.9250	1.3484
10	.9330	1.3601
15	.9270	1.3513
20	.9110	1.3280
25	.8880	1.2945
30	.8460	1.2332
45	.7570	1.1035
60	.7060	1.0292
75	.6600	.9621
90	.6590	.9606

TWO SPECULAR REFLECTIONS

ANGLE OF ATTACK	$K(G,S,A)$	$K(G,S,A)/K(G,0,0)$
0	.9150	1.3338
5	.9180	1.3382
10	.9110	1.3280
15	.8920	1.3003
20	.9170	1.3367
25	.9310	1.3571
30	.9260	1.3499
45	.8360	1.2187
60	.7380	1.0758
75	.6810	.9927
90	.6570	.9577

TABLE 14

TRANSMISSION PROBABILITIES FOR THE VACUUM
GAUGES ON THE EXPLORER XVII AND EXPLORER XXXII
AERONOMY SATELLITES

SPEED RATIO = 7.5 $K(G,0,0) = .686$
BAYARD-ALPERT GAUGE

NO SPECULAR REFLECTIONS

ANGLE OF ATTACK	$K(G,S,A)$	$K(G,S,A)/K(G,0,0)$
0	.9100	1.3265
5	.8940	1.3032
10	.8500	1.2391
15	.7910	1.1531
20	.7490	1.0918
25	.7240	1.0554
30	.6950	1.0131
45	.6700	.9767
60	.6670	.9723
75	.6590	.9606
90	.6700	.9767

ONE SPECULAR REFLECTION

ANGLE OF ATTACK	$K(G,S,A)$	$K(G,S,A)/K(G,0,0)$
0	.9150	1.3338
5	.9180	1.3382
10	.9340	1.3615
15	.9280	1.3528
20	.9120	1.3294
25	.8860	1.2915
30	.8530	1.2434
45	.7460	1.0875
60	.7060	1.0292
75	.6550	.9548
90	.6610	.9636

TWO SPECULAR REFLECTIONS

ANGLE OF ATTACK	$K(G,S,A)$	$K(G,S,A)/K(G,0,0)$
0	.9170	1.3367
5	.9170	1.3367
10	.9130	1.3309
15	.8960	1.3061
20	.9110	1.3280
25	.9280	1.3528
30	.9250	1.3484
45	.8430	1.2289
60	.7550	1.1006
75	.6820	.9942
90	.6140	.8950

TABLE 15

TRANSMISSION PROBABILITIES FOR THE VACUUM
GAUGES ON THE EXPLORER XVII AND EXPLORER XXXII
AERONOMY SATELLITES

SPEED RATIO = 8.0 $K(G,0,0) = .686$
BAYARD-ALPERT GAUGE

NO SPECULAR REFLECTIONS

ANGLE OF ATTACK	$K(G,S,A)$	$K(G,S,A)/K(G,0,0)$
0	.9140	1.3324
5	.9000	1.3120
10	.8520	1.2420
15	.7910	1.1531
20	.7430	1.0831
25	.7150	1.0423
30	.7000	1.0204
45	.6670	.9723
60	.6590	.9606
75	.6590	.9606
90	.6650	.9694

ONE SPECULAR REFLECTION

ANGLE OF ATTACK	$K(G,S,A)$	$K(G,S,A)/K(G,0,0)$
0	.8970	1.3076
5	.9200	1.3411
10	.9390	1.3688
15	.9240	1.3469
20	.9170	1.3367
25	.8930	1.3017
30	.8480	1.2362
45	.7560	1.1020
60	.7140	1.0408
75	.6600	.9621
90	.6600	.9621

TWO SPECULAR REFLECTIONS

ANGLE OF ATTACK	$K(G,S,A)$	$K(G,S,A)/K(G,0,0)$
0	.9180	1.3382
5	.9180	1.3382
10	.9110	1.3280
15	.8890	1.2959
20	.9130	1.3309
25	.9340	1.3615
30	.9290	1.3542
45	.8400	1.2245
60	.7400	1.0787
75	.6880	1.0029
90	.6690	.9752

TABLE 16

TRANSMISSION PROBABILITIES FOR THE VACUUM
GAUGES ON THE EXPLORER XVII AND EXPLORER XXXII
AERONOMY SATELLITES

SPEED RATIO = 9.0 $K(G,0,0) = .686$
BAYARD-ALPERT GAUGE

NO SPECULAR REFLECTIONS

ANGLE OF ATTACK	$K(G,S,A)$	$K(G,S,A)/K(G,0,0)$
0	.9210	1.3426
5	.9150	1.3338
10	.8560	1.2478
15	.7930	1.1560
20	.7420	1.0816
25	.7190	1.0481
30	.7070	1.0306
45	.6730	.9810
60	.6610	.9636
75	.6580	.9592
90	.6690	.9752

ONE SPECULAR REFLECTION

ANGLE OF ATTACK	$K(G,S,A)$	$K(G,S,A)/K(G,0,0)$
0	.8750	1.2755
5	.9140	1.3324
10	.9430	1.3746
15	.9260	1.3499
20	.9170	1.3367
25	.9000	1.3120
30	.8520	1.2420
45	.7610	1.1093
60	.7000	1.0204
75	.6590	.9606
90	.6590	.9606

TWO SPECULAR REFLECTIONS

ANGLE OF ATTACK	$K(G,S,A)$	$K(G,S,A)/K(G,0,0)$
0	.9160	1.3353
5	.9190	1.3397
10	.9110	1.3280
15	.8870	1.2930
20	.9200	1.3411
25	.9410	1.3717
30	.9280	1.3528
45	.8340	1.2157
60	.7470	1.0889
75	.6810	.9927
90	.6620	.9650

TRANSMISSION PROBABILITIES FOR THE VACUUM
 GAUGES ON THE EXPLORER XVII AND EXPLORER XXXII
 AERONOMY SATELLITES

REDHEAD GAUGE

O NO SPECULAR REFLECTIONS

I ONE SPECULAR REFLECTION

X TWO SPECULAR REFLECTIONS

SPEED RATIO = 2.0

K(G, S, Q)

.70

.65

.60

.55

.50

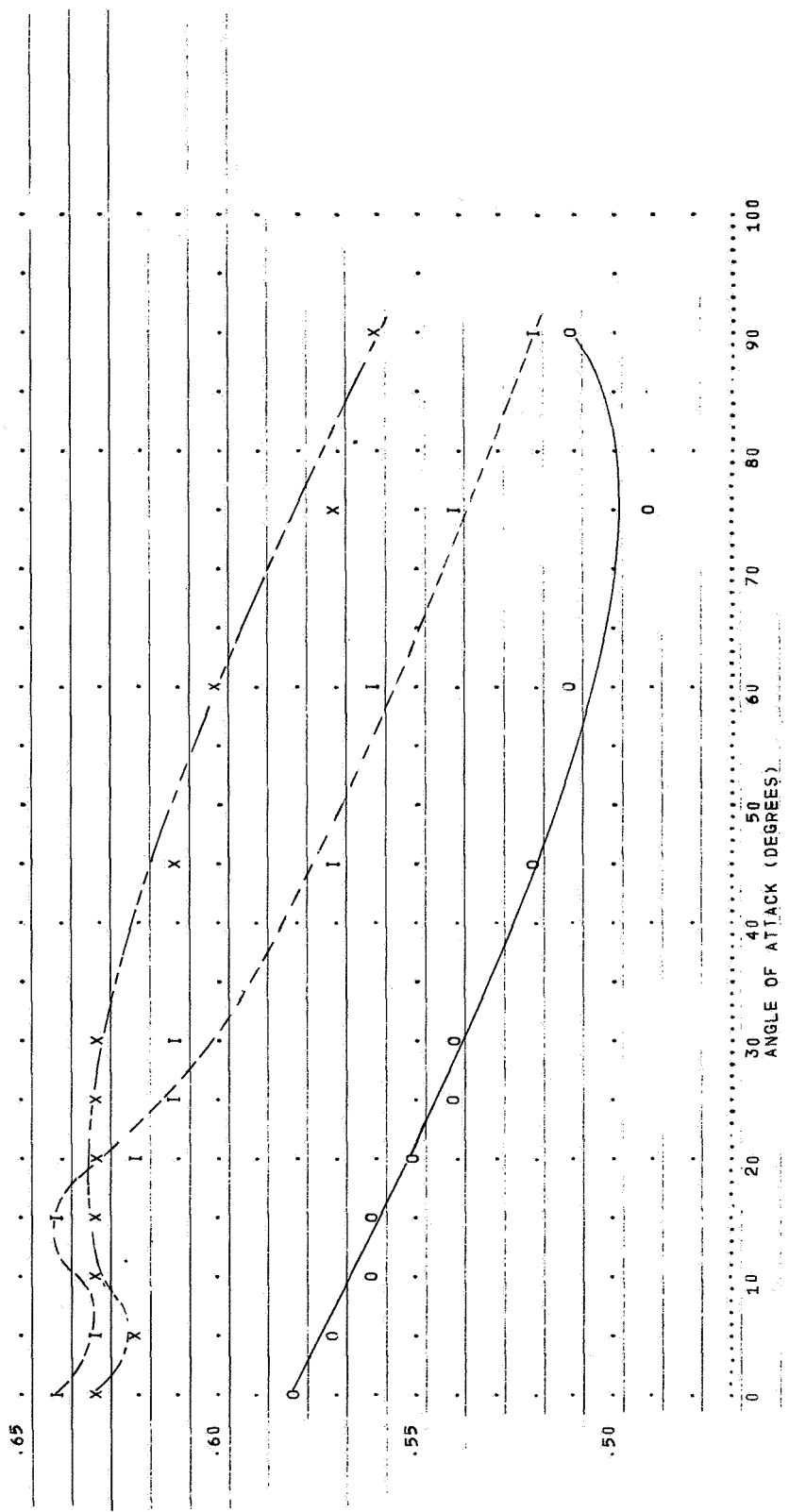


FIGURE 1

TRANSMISSION PROBABILITIES FOR THE VACUUM
GAUGES ON THE EXPLORER XVII AND EXPLORER XXXII
AERONOMY SATELLITES

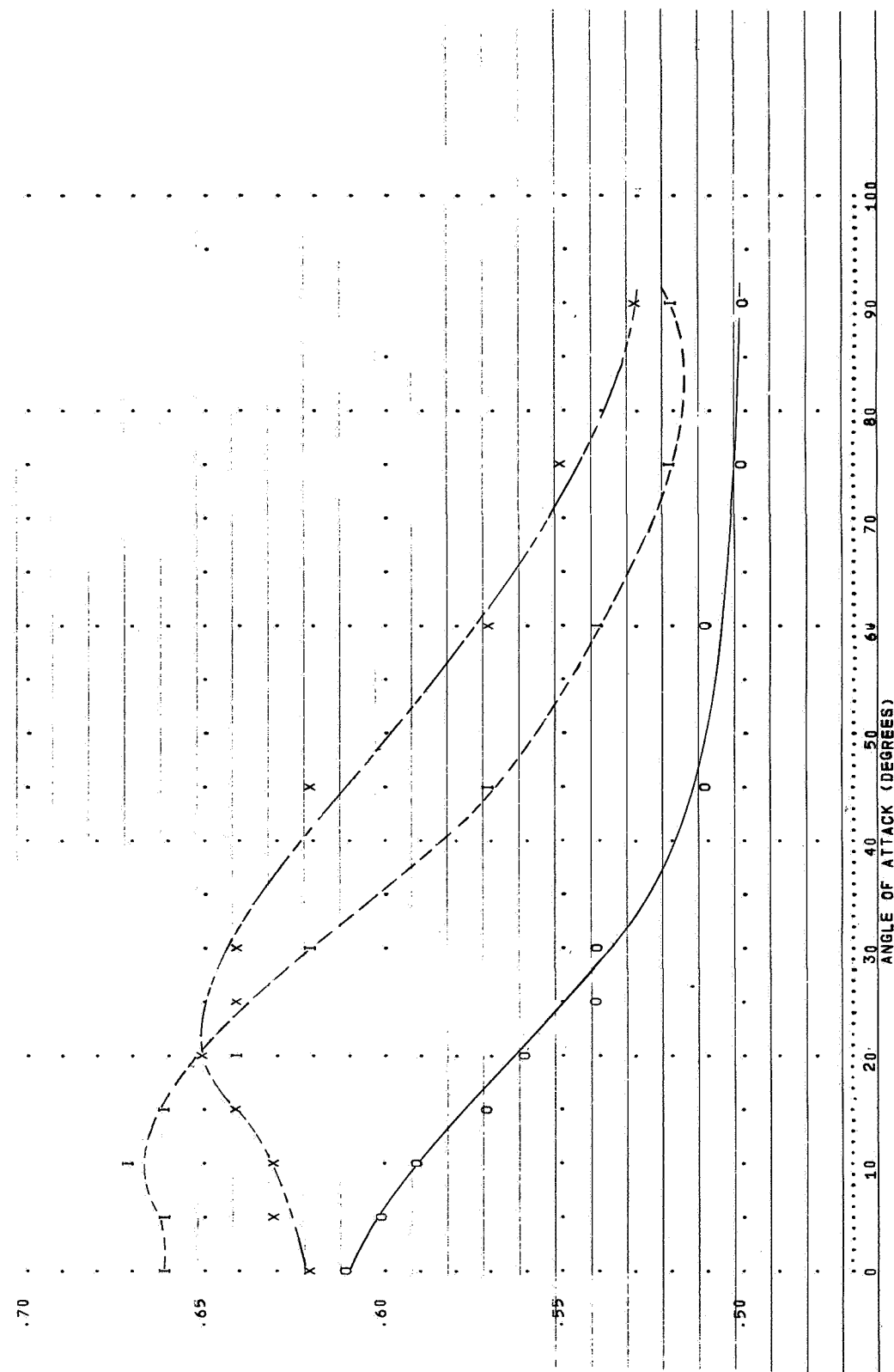


FIGURE 2

TRANSMISSION PROBABILITIES FOR THE VACUUM
GAUGES ON THE EXPLORER XVII AND EXPLORER XXXIII
AERONAUTICS SATELLITES

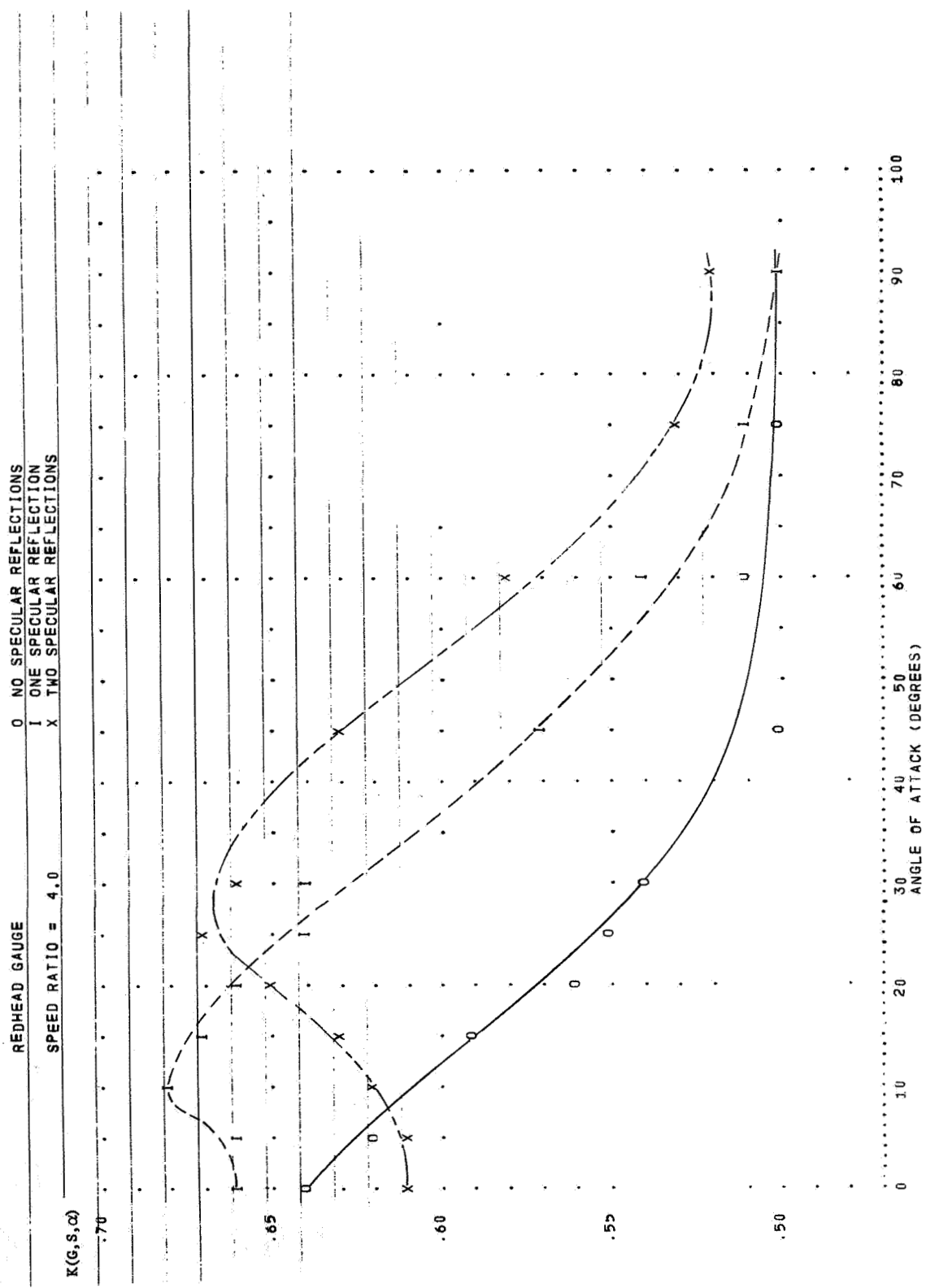


FIGURE 3

TRANSMISSION PROBABILITIES FOR THE VACUUM
GAUGES ON THE EXPLORER XVII AND EXPLORER XXXII
AERONAUTICSATELLITES

REDHEAD GAUGE	0	NO SPECULAR REFLECTIONS
SPEED RATIO =	1	ONE SPECULAR REFLECTION
	x	TWO SPECULAR REFLECTIONS

$K(G, S, \alpha)$

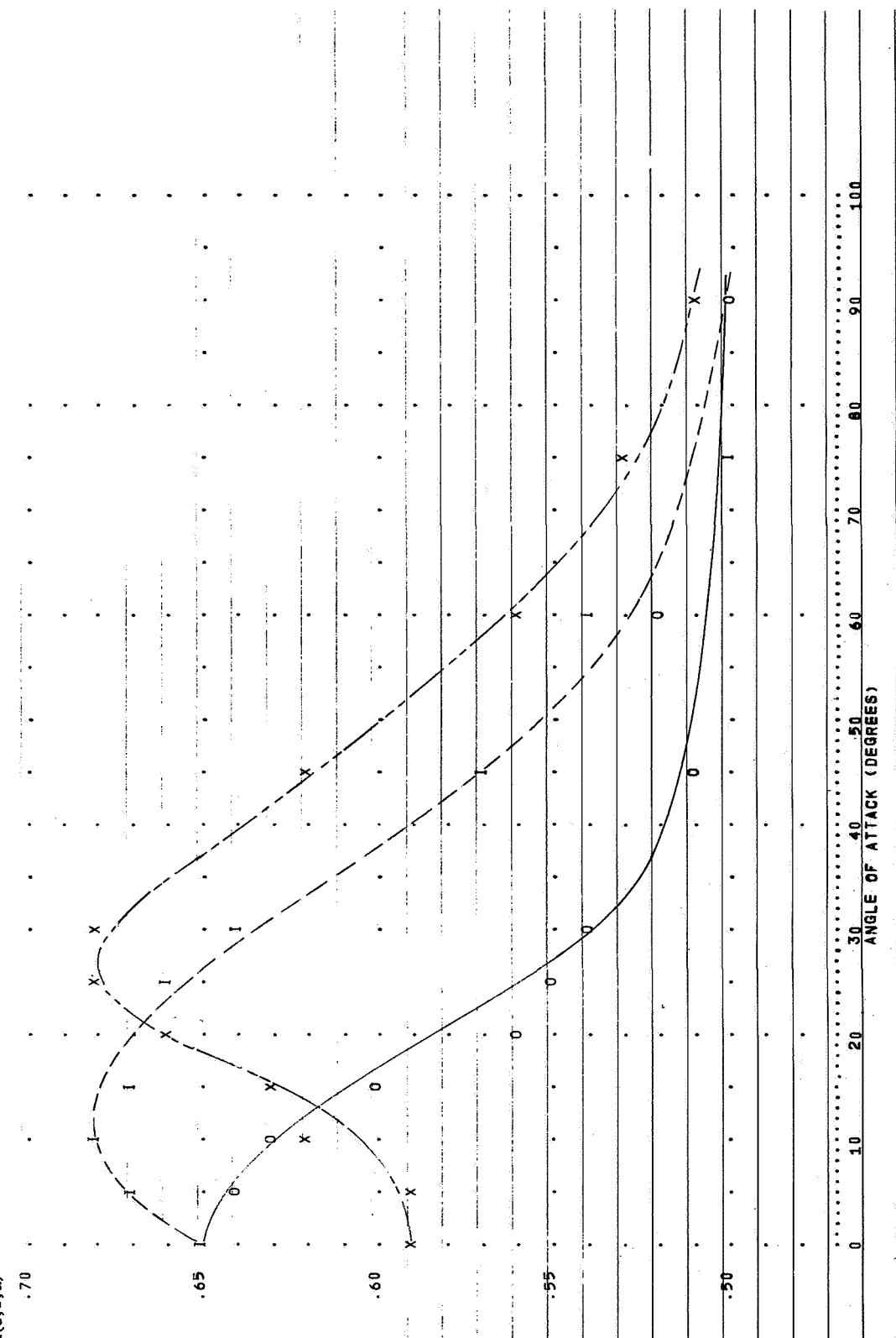


FIGURE 4

TRANSMISSION PROBABILITIES FOR THE VACUUM
GAUGES ON THE EXPLORER XVI AND EXPLORER XXXII
AERONOMY SATELLITES

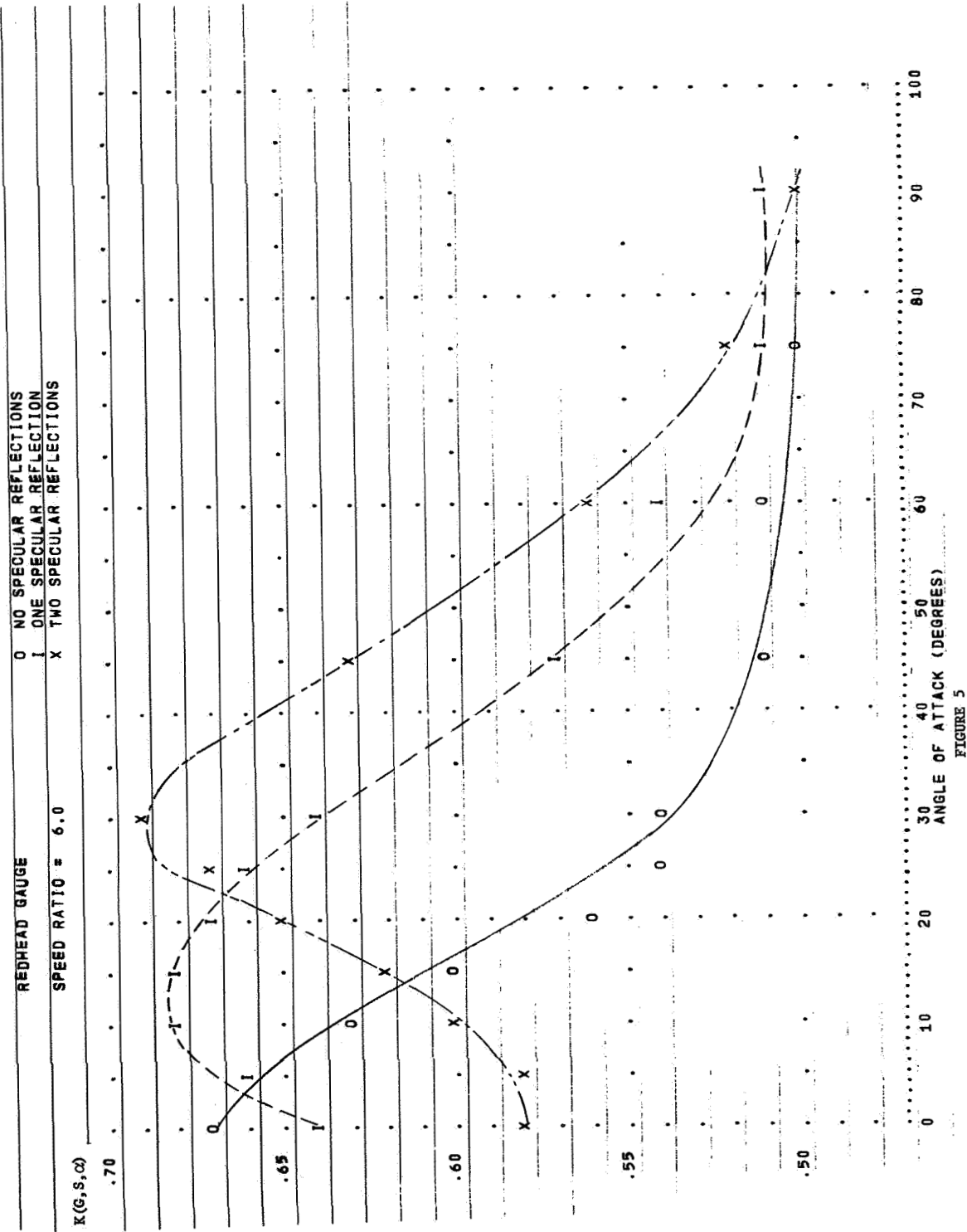


FIGURE 5

TRANSMISSION PROBABILITIES FOR THE VACUUM
GAUGES ON THE EXPLORER XVII AND EXPLORER XXXII
AERONOMY SATELLITES

REDHEAD GAUGE
SPEED RATIO = 7.0
 $K(G, S, \omega)$

0 NO SPECULAR REFLECTIONS
1 ONE SPECULAR REFLECTION
X TWO SPECULAR REFLECTIONS

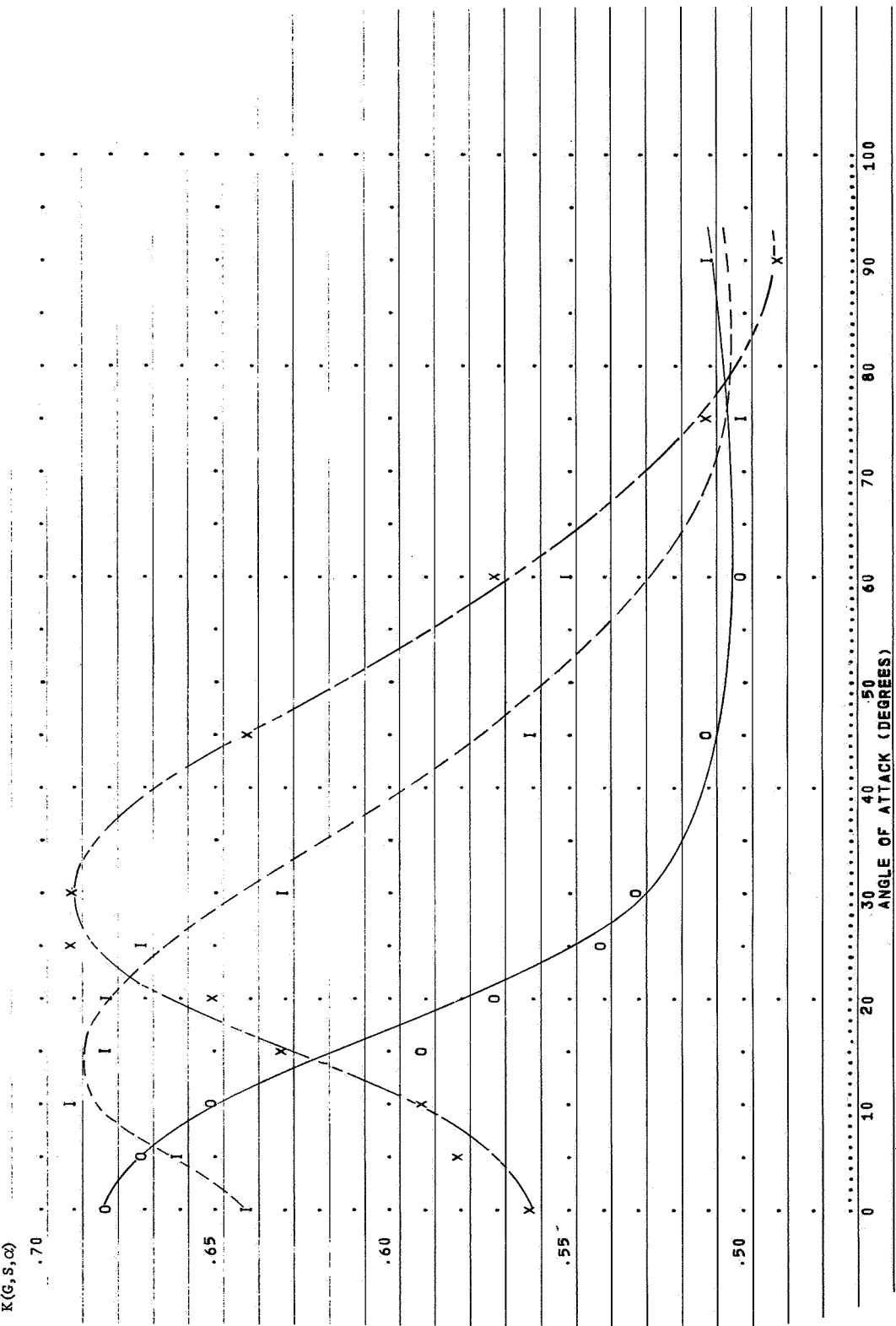


FIGURE 6

TRANSMISSION PROBABILITIES FOR THE VACUUM
GAUGES ON THE EXPLORER XVII AND EXPLORER XXXII
AERONAUTICS SATELLITES

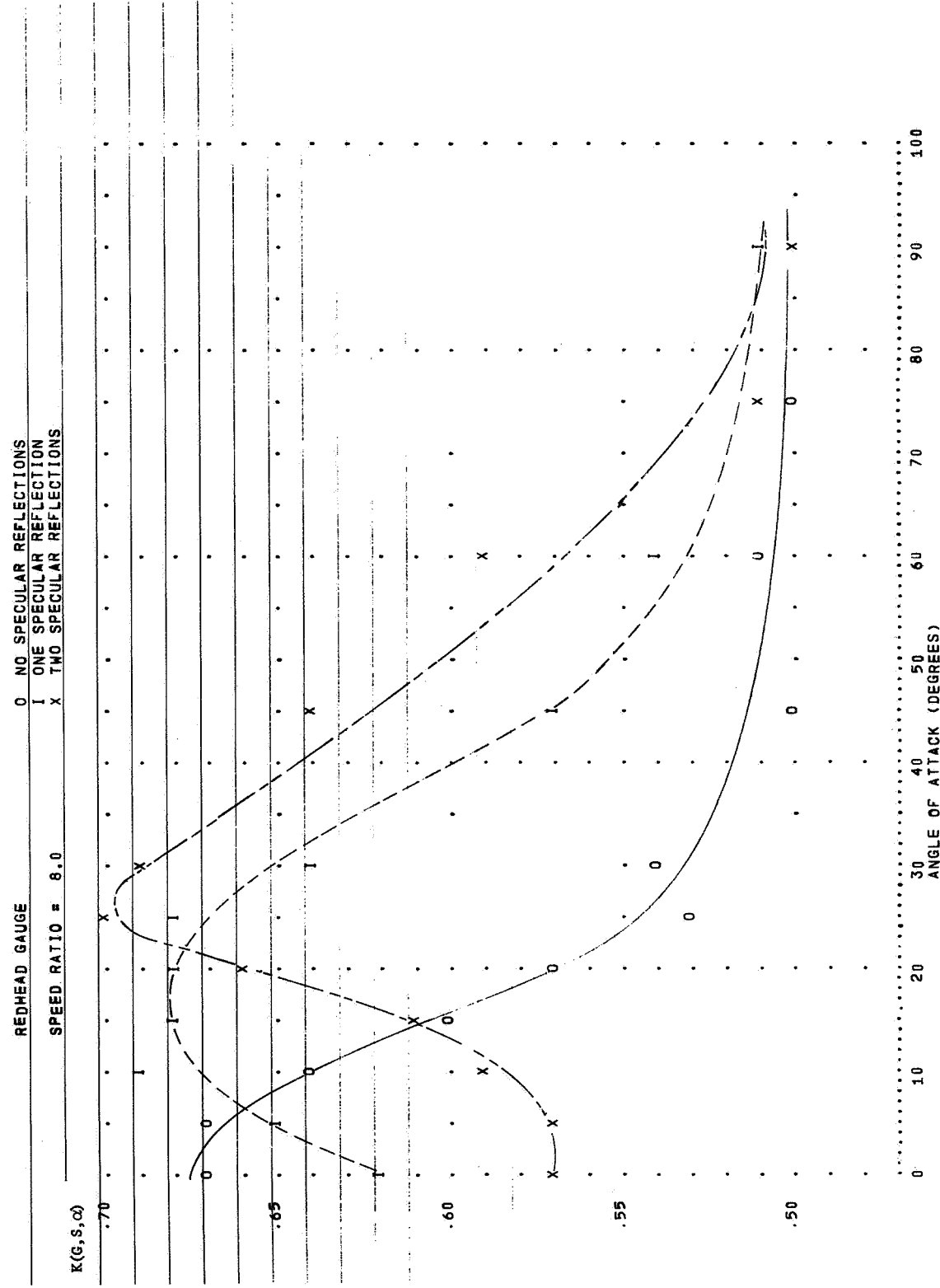


FIGURE 7

THEORETICAL PRESSURE RATIO RESPONSE FOR
THE VACUUM GAUGES ON THE EXPLORER XVII
AND EXPLORER XXXII AERONAUTICS SATELLITES

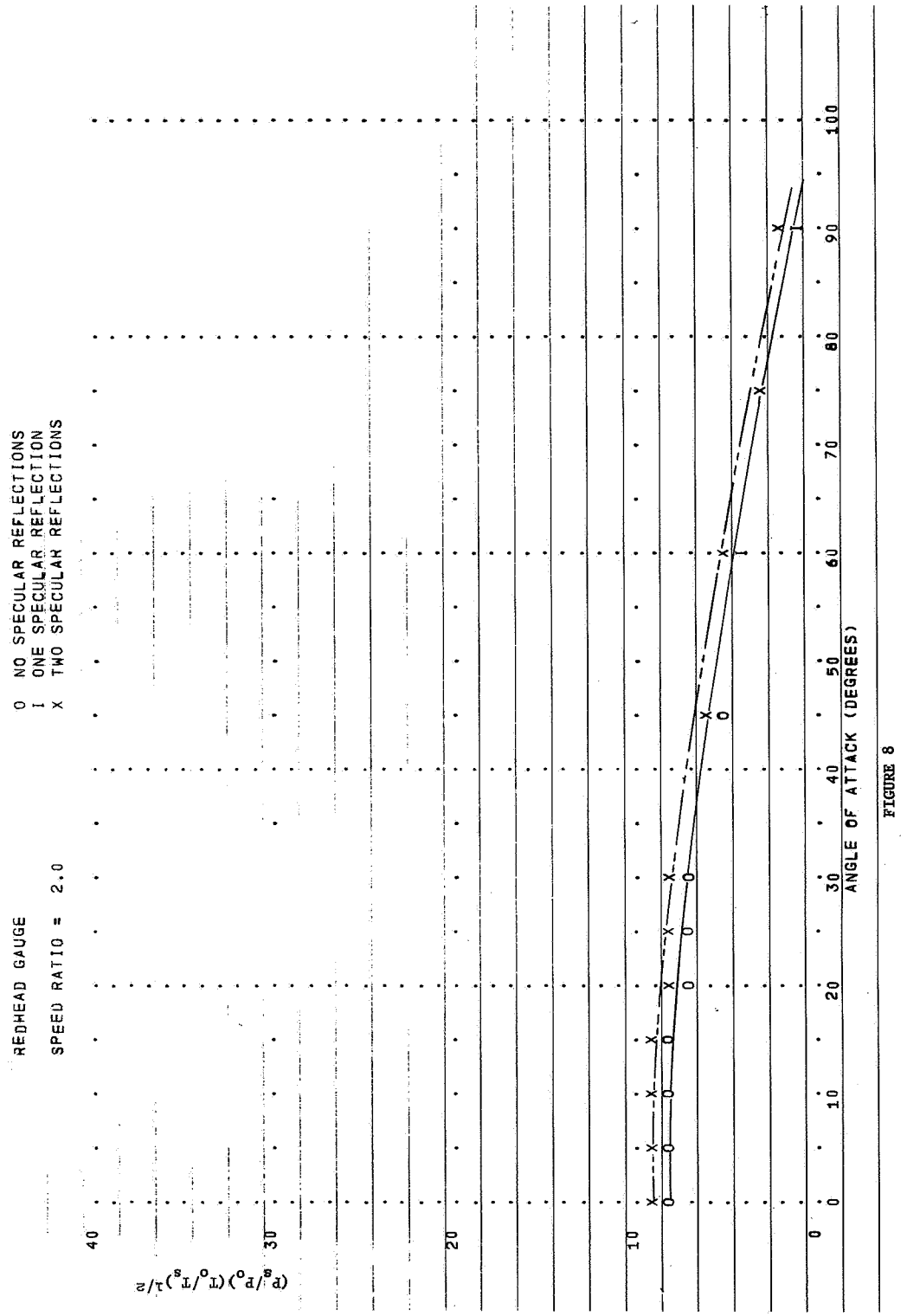


FIGURE 8

THEORETICAL PRESSURE RATIO RESPONSE FOR
THE VACUUM GAUGES ON THE EXPLORER XVII
AND EXPLORER XXXII AERONOMY SATELLITES

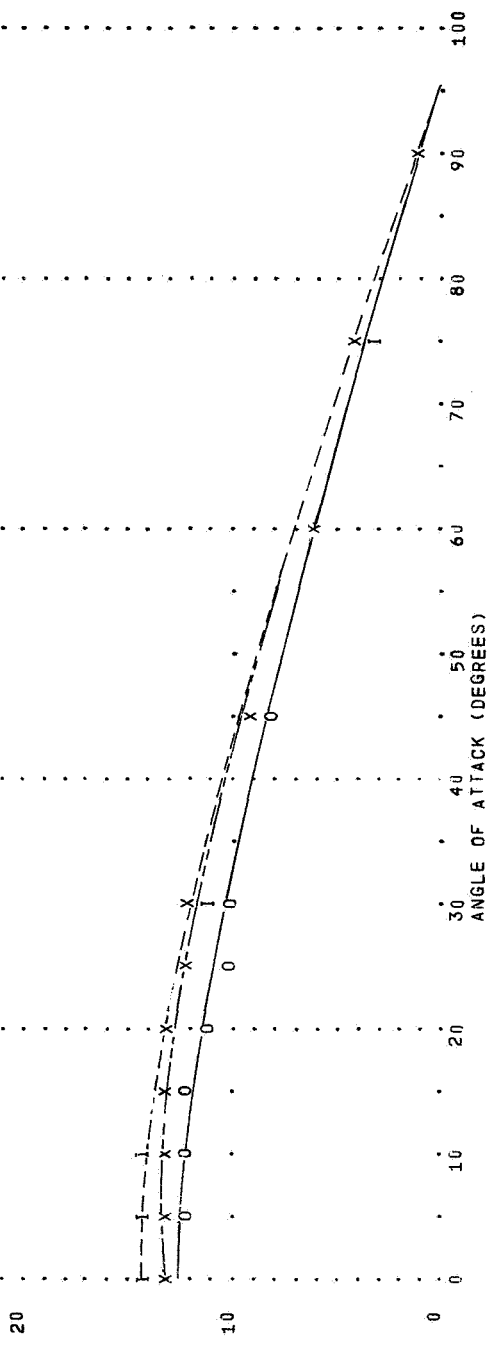
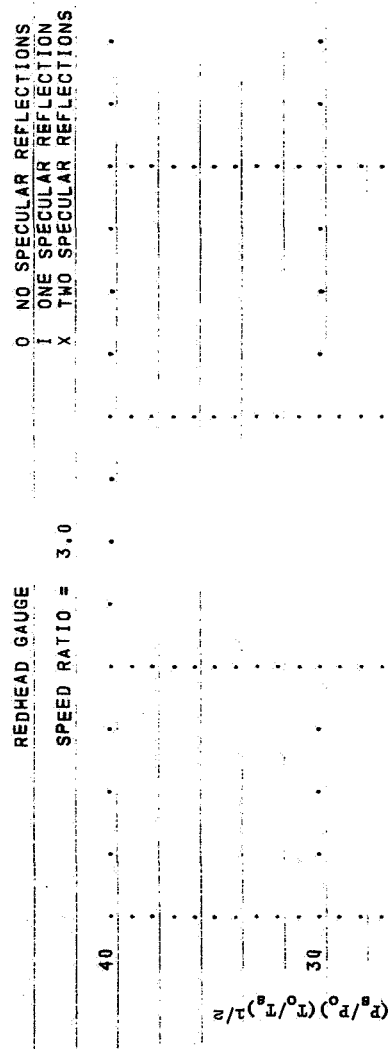


FIGURE 9

THEORETICAL PRESSURE RATIO RESPONSE FOR
THE VACUUM GAUGES ON THE EXPLORER XVI
AND EXPLORER XXXII AERONAUTICSATELLITES

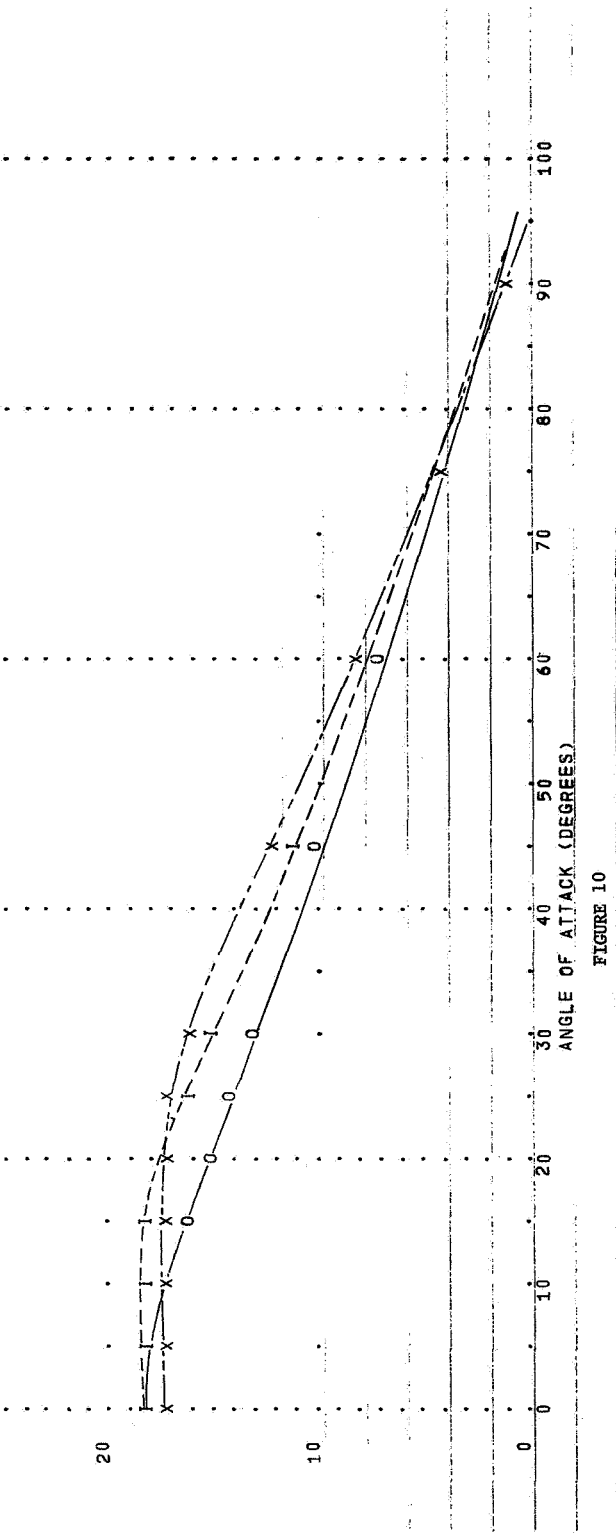
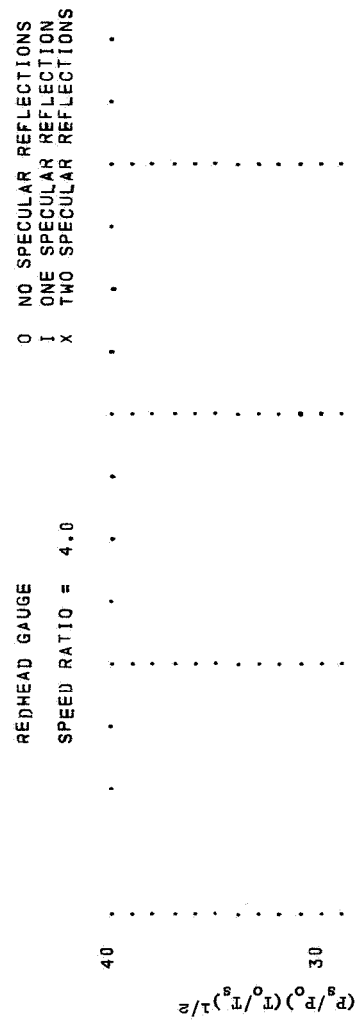


FIGURE 10

THEORETICAL PRESSURE RATIO RESPONSE FOR
THE VACUUM GAUGES ON THE EXPLORER XVII
AND EXPLORER XXXII AERONOMY SATELLITES

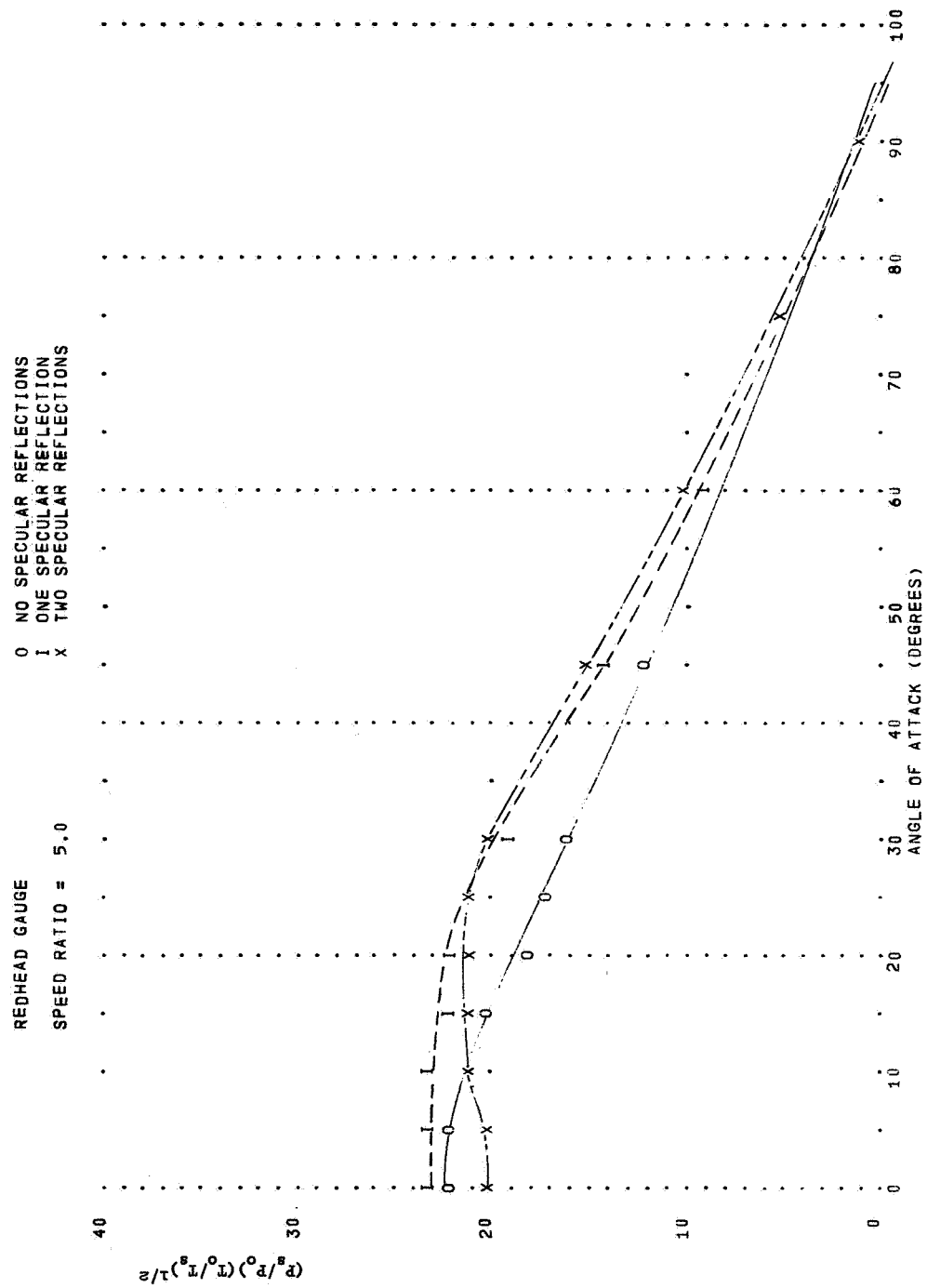


FIGURE 11.

THEORETICAL PRESSURE RATIO RESPONSE FOR
THE VACUUM GAUGES ON THE EXPLORER XVII
AND EXPLORER XXXII AERONAUTICS SATELLITES

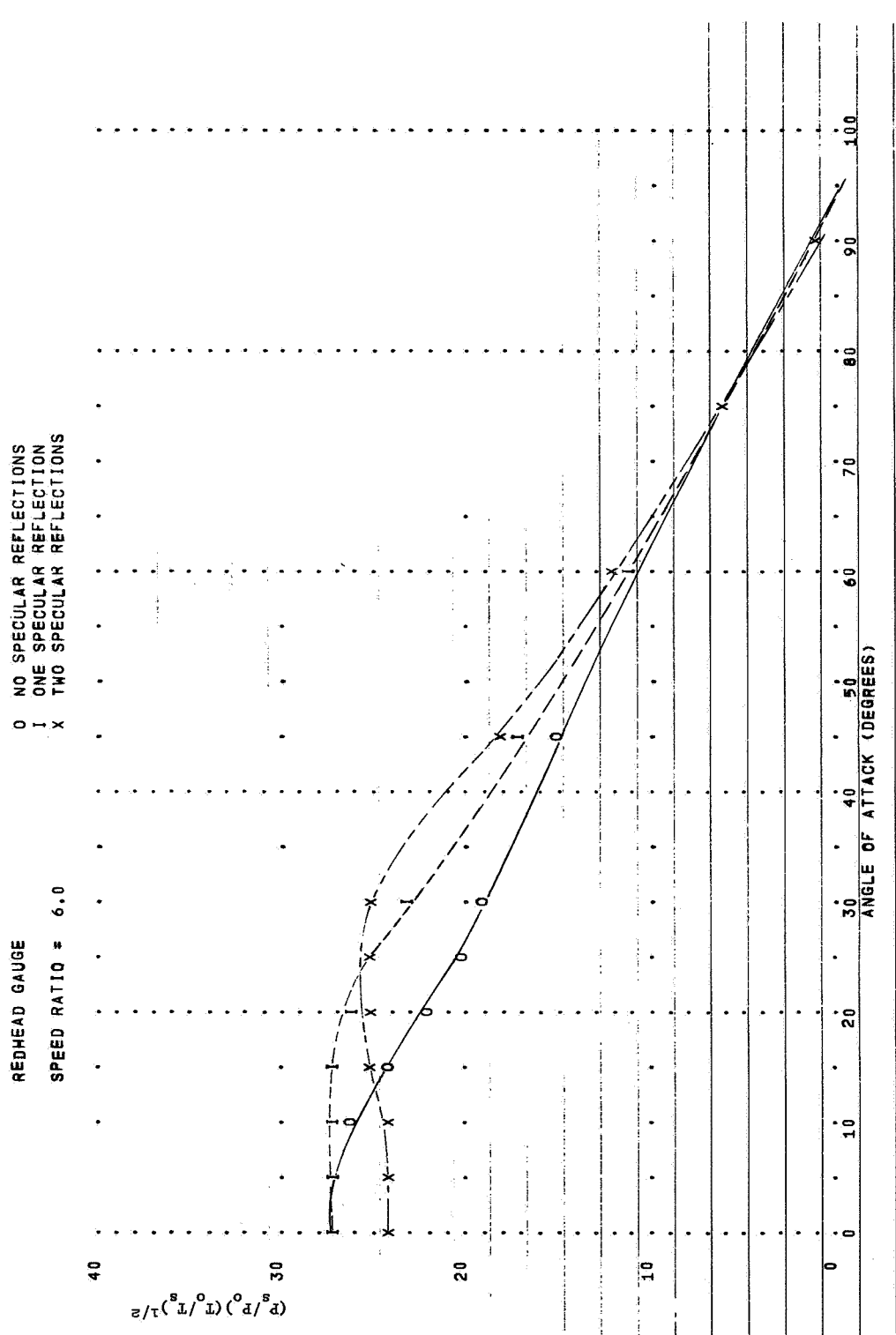


FIGURE 12

THEORETICAL PRESSURE RATIO RESPONSE FOR
THE VACUUM GAUGES ON THE EXPLORER XVII
AND EXPLORER XXXII AERONOMY SATELLITES

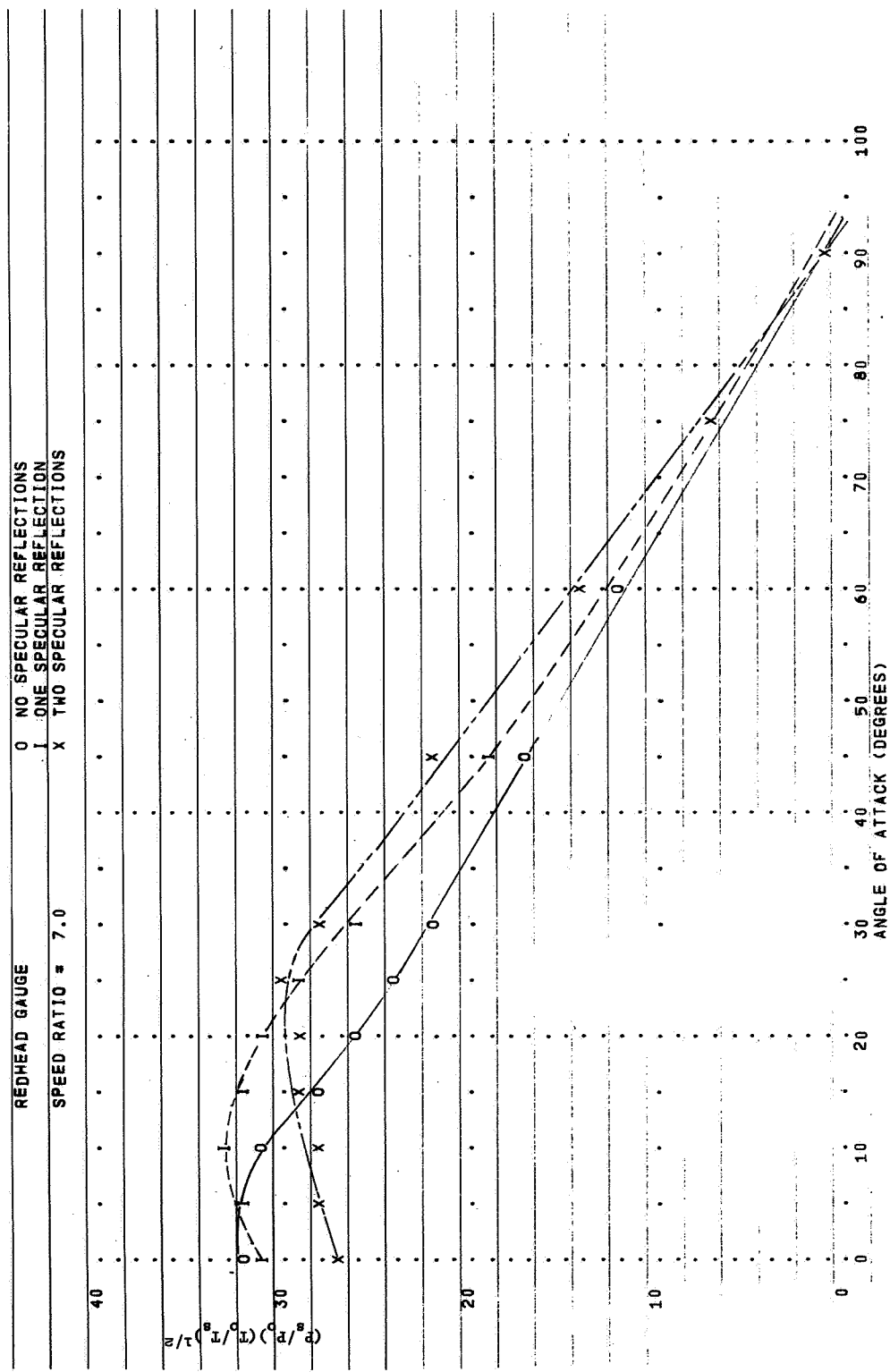


FIGURE 13

THEORETICAL PRESSURE RATIO RESPONSE FOR
THE VACUUM GAUGES ON THE EXPLORER XVII
AND EXPLORER XXXII AERONOMY SATELLITES

REDHEAD GAUGE 0 NO SPECULAR REFLECTIONS
 SPEED RATIO = 8.0 1 ONE SPECULAR REFLECTION
 X TWO SPECULAR REFLECTIONS

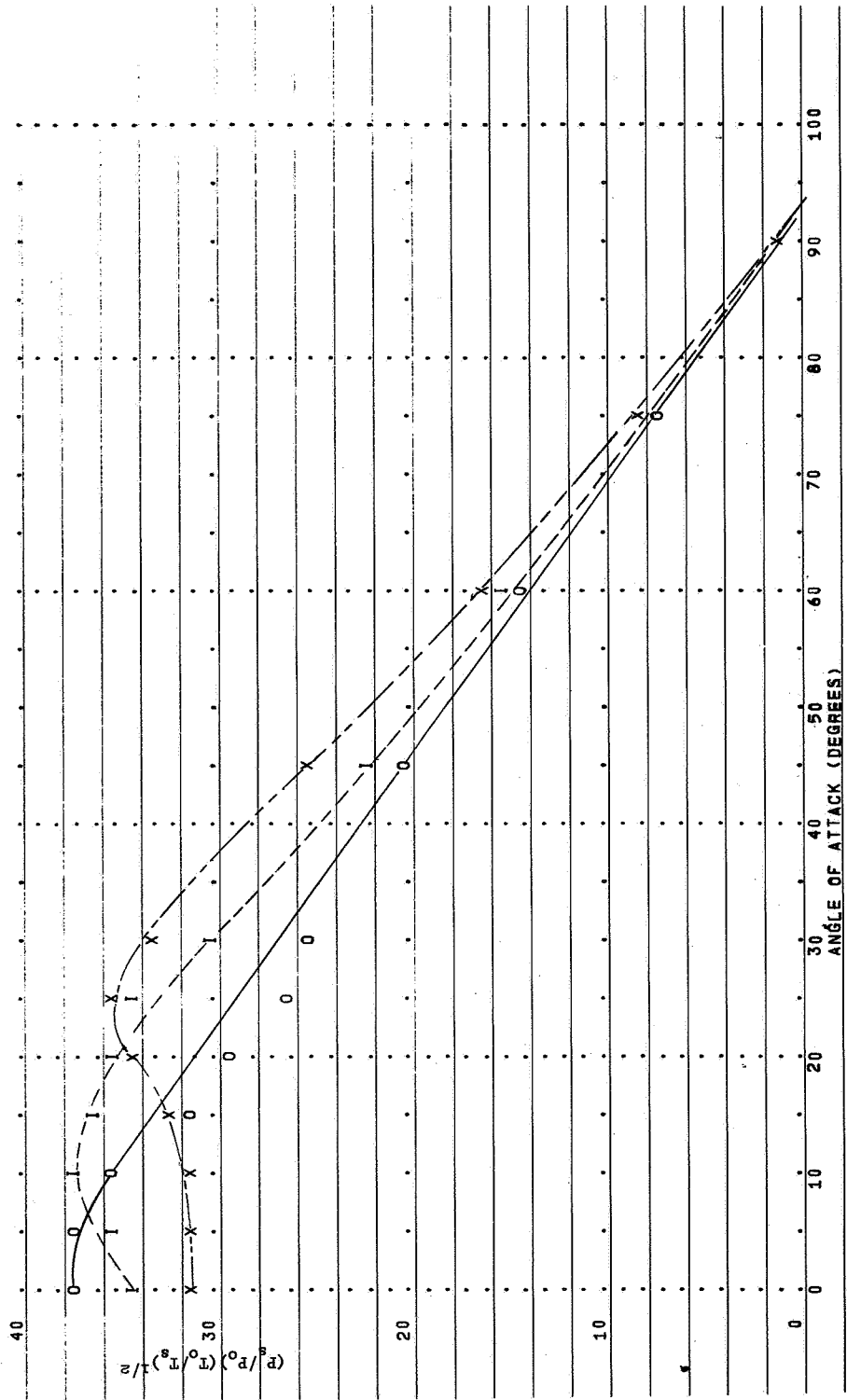


FIGURE 14

TRANSMISSION PROBABILITIES FOR THE VACUUM
GAUGES ON THE EXPLORER XVII AND EXPLORER XXXII
AERONAUTICS SATELLITES

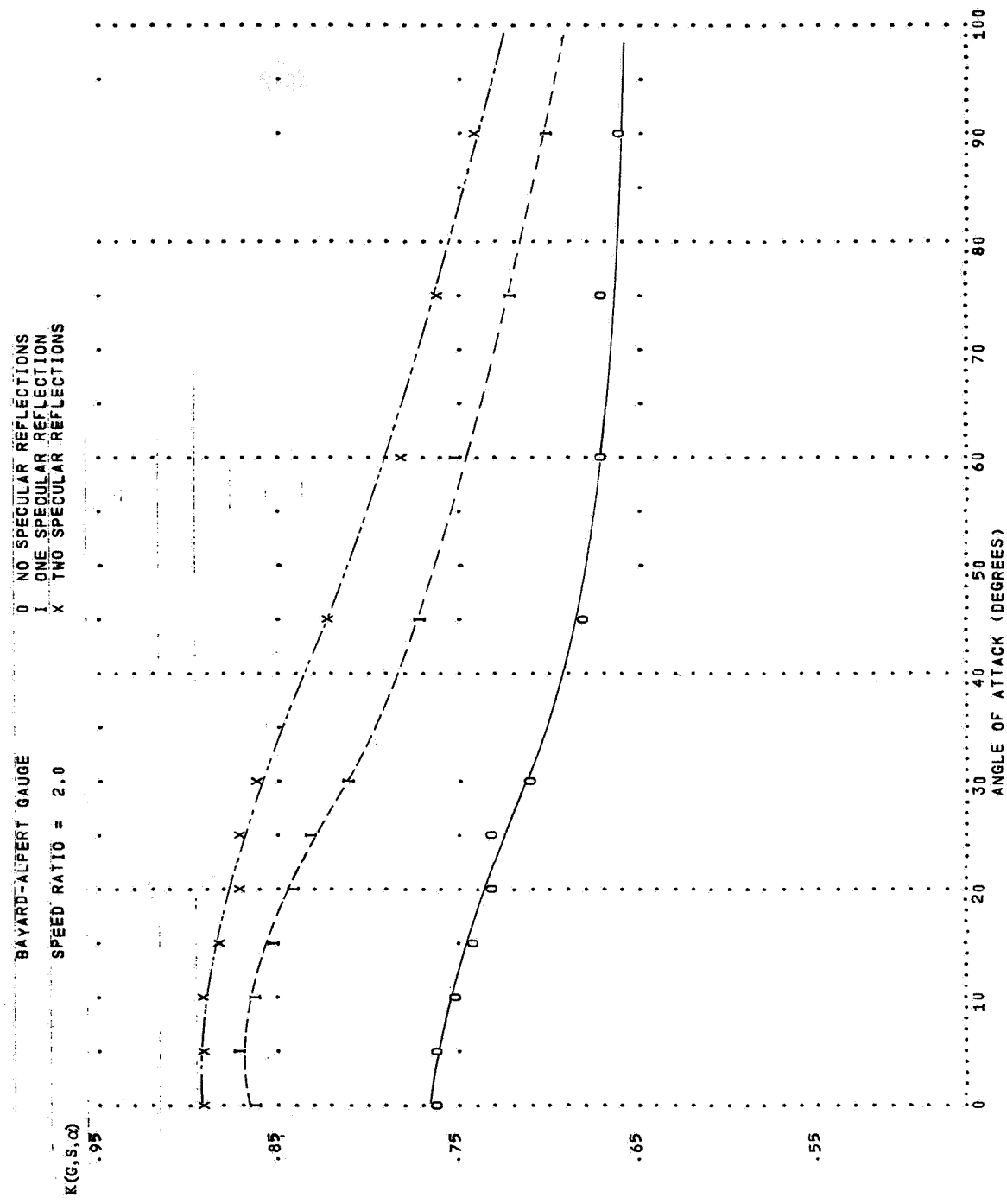


FIGURE 15

TRANSMISSION PROBABILITIES FOR THE VACUUM
GAUGES ON THE EXPLORER XVII AND EXPLORER XXXII
AERONOMY SATELLITES

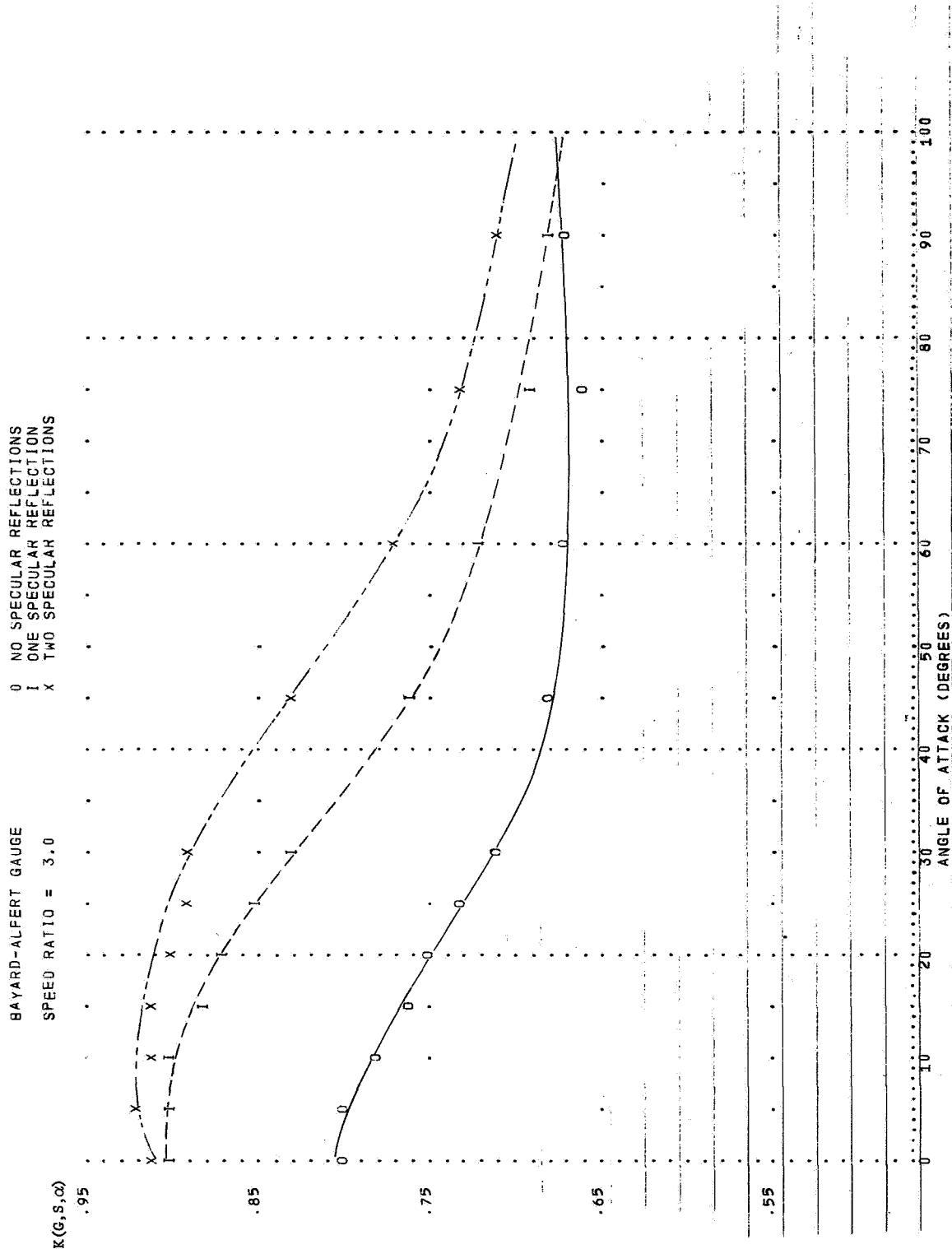


FIGURE 16

TRANSMISSION PROBABILITIES FOR THE VACUUM
GAUGES ON THE EXPLORER XVII AND EXPLORER XXXII
AERONOMY SATELLITES

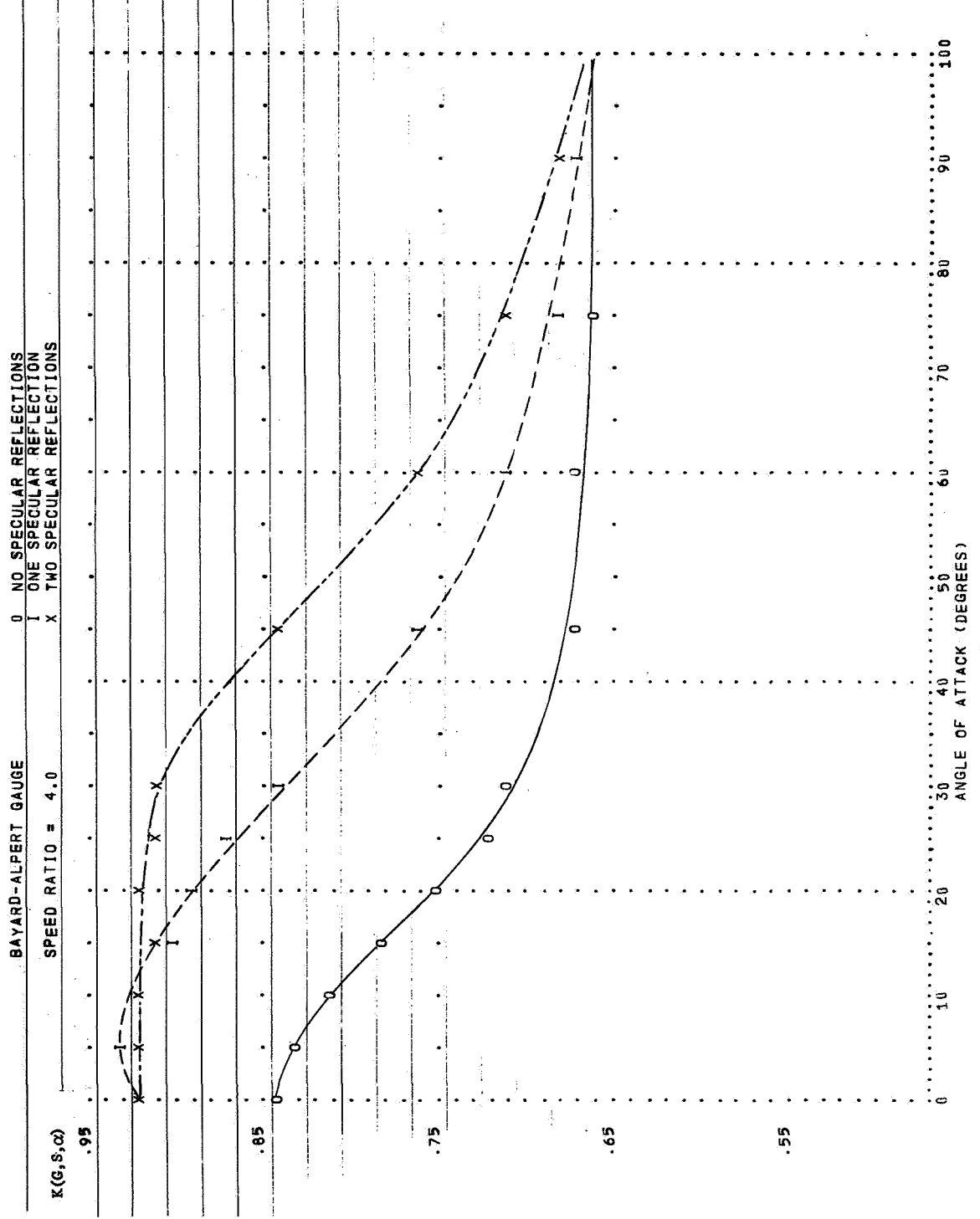


FIGURE 17

TRANSMISSION PROBABILITIES FOR THE VACUUM
GAUGES ON THE EXPLORER XVII AND EXPLORER XXXII
AERONOMY SATELLITES

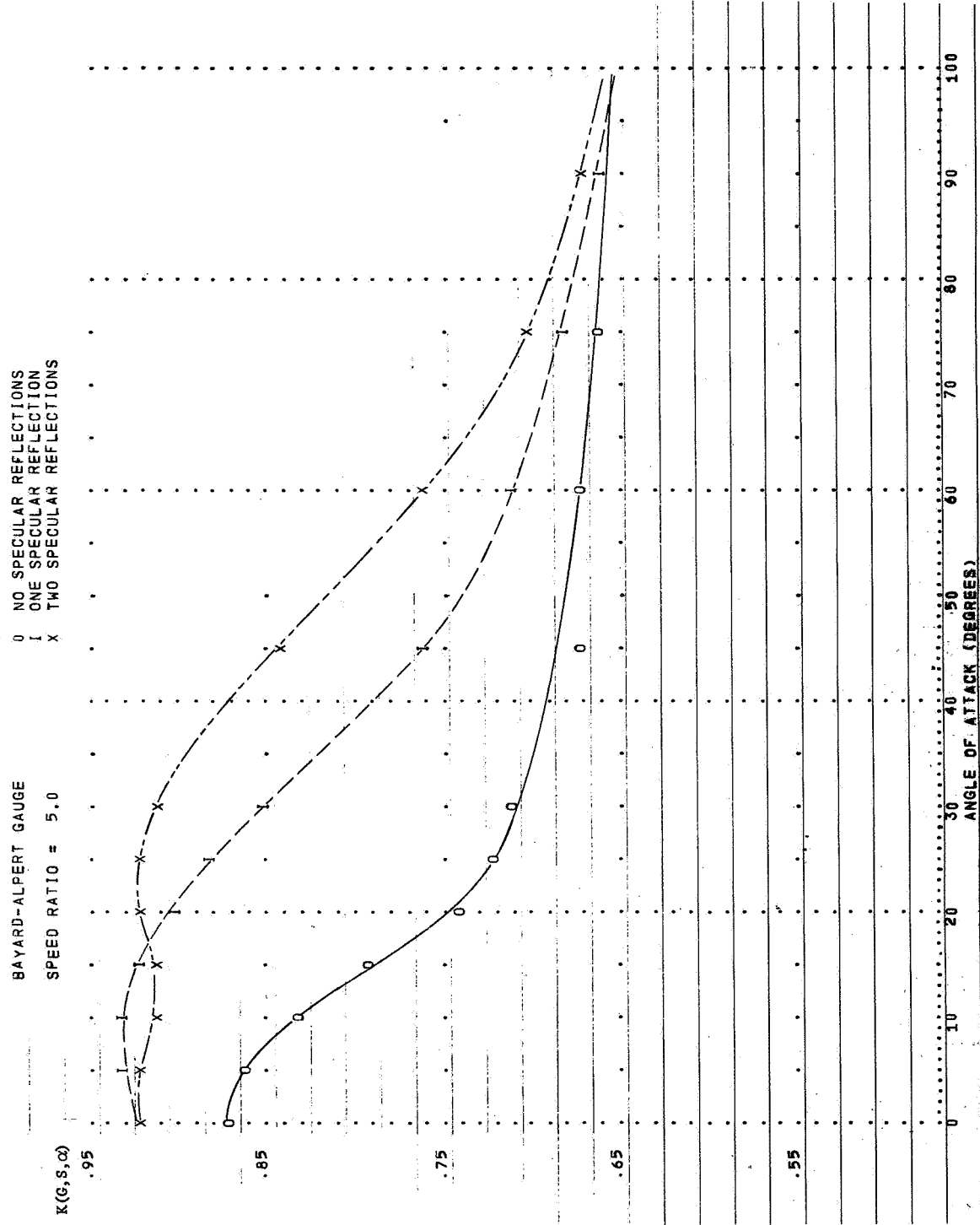


FIGURE 18

TRANSMISSION PROBABILITIES FOR THE VACUUM
GAUGES ON THE EXPLORER XVII AND EXPLORER XXXII
AERODYNAMIC SATELLITES

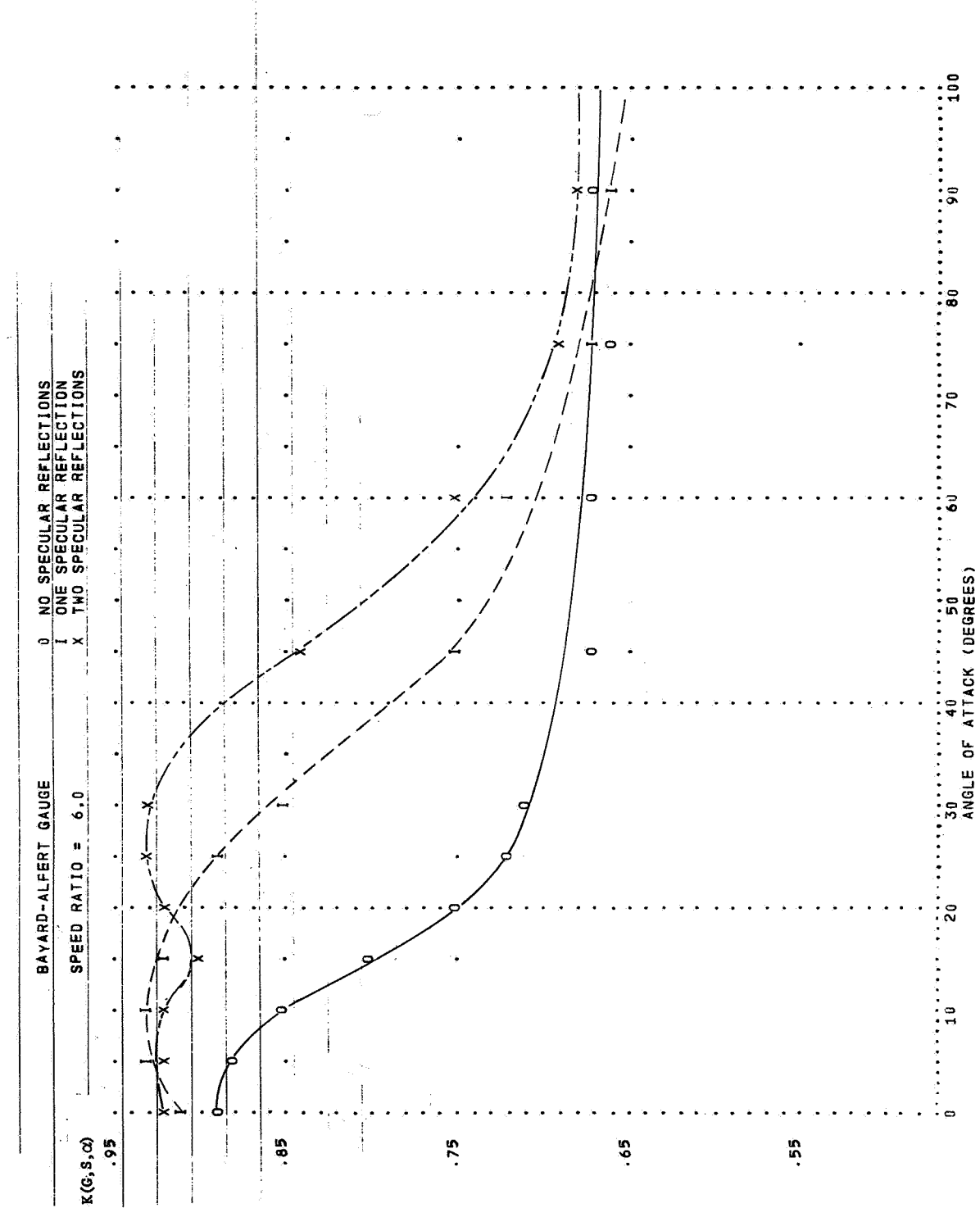


FIGURE 19

TRANSMISSION PROBABILITIES FOR THE VACUUM
GAUGES ON THE EXPLORER XVII AND EXPLORER XXXII
AERONOMY SATELLITES

BAYARD-ALPERT GAUGE
SPEED RATIO = 7.0

0 NO SPECULAR REFLECTIONS

1 ONE SPECULAR REFLECTION

X TWO SPECULAR REFLECTIONS

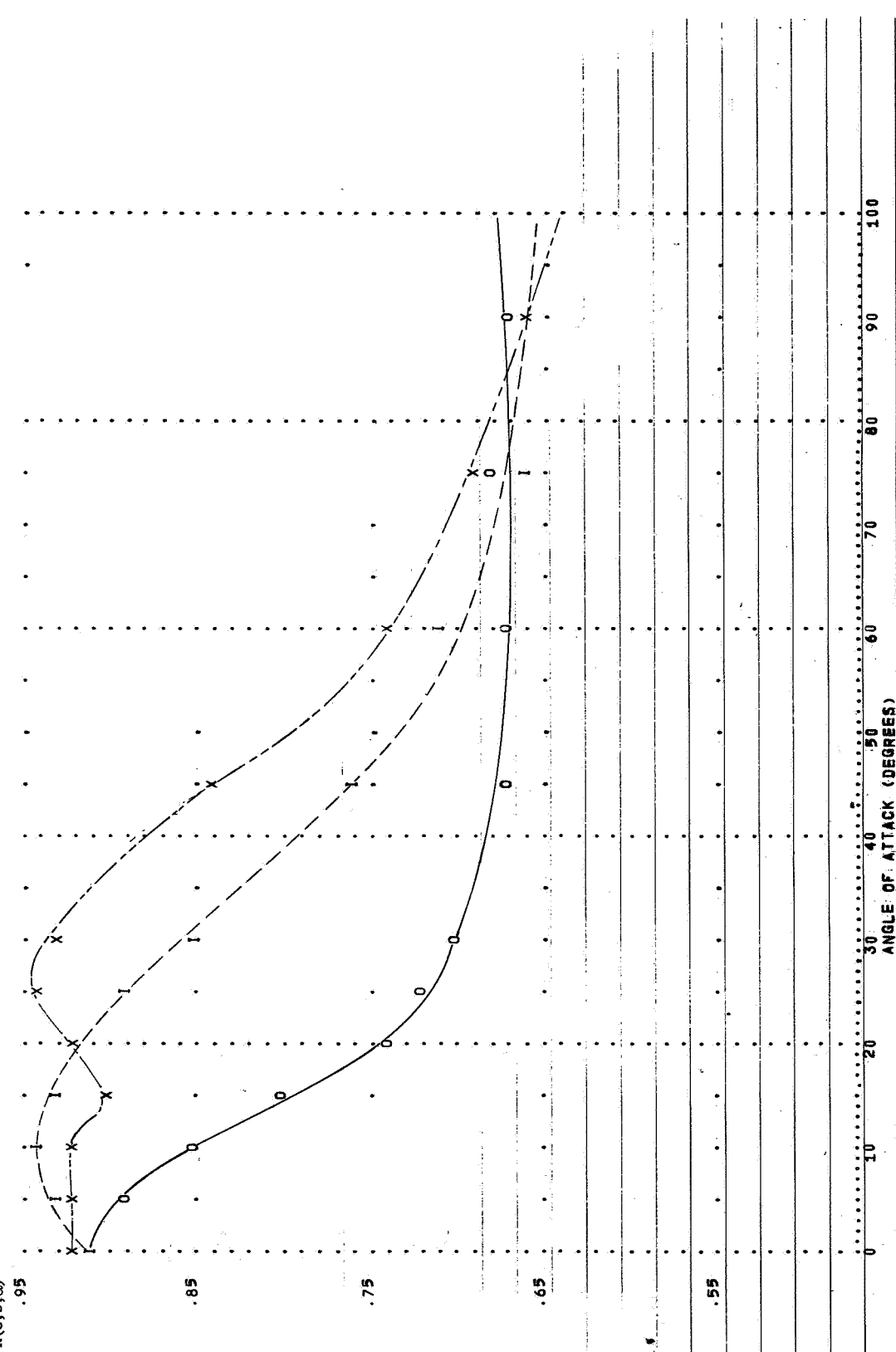


FIGURE 20

TRANSMISSION PROBABILITIES FOR THE VACUUM
GAUGES ON THE EXPLORER XVII AND EXPLORER XXXII
AERONOMY SATELLITES

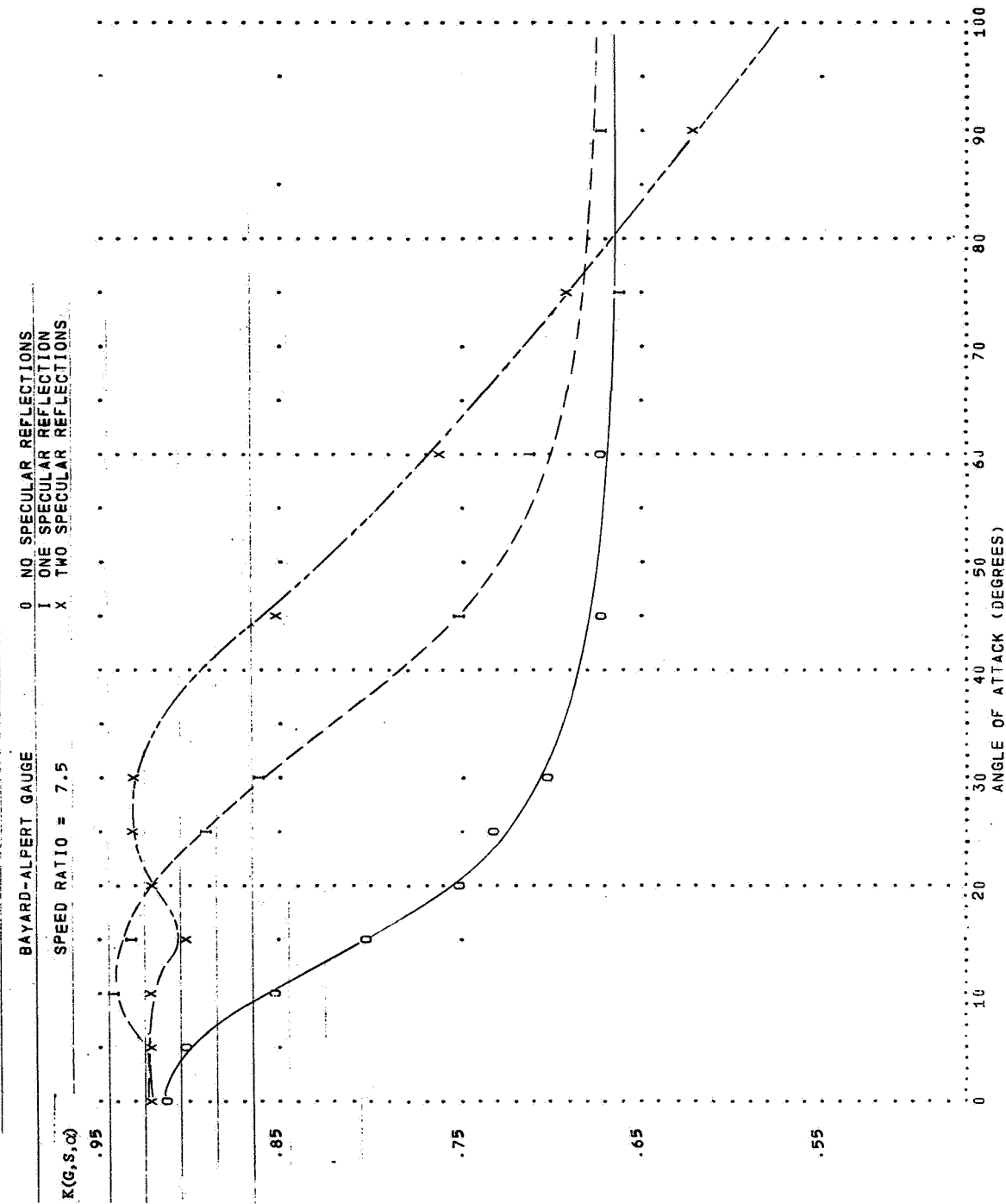


FIGURE 21

TRANSMISSION PROBABILITIES FOR THE VACUUM
GAUGES ON THE EXPLORER XVII AND EXPLORER XXXI
AERONOMY SATELLITES

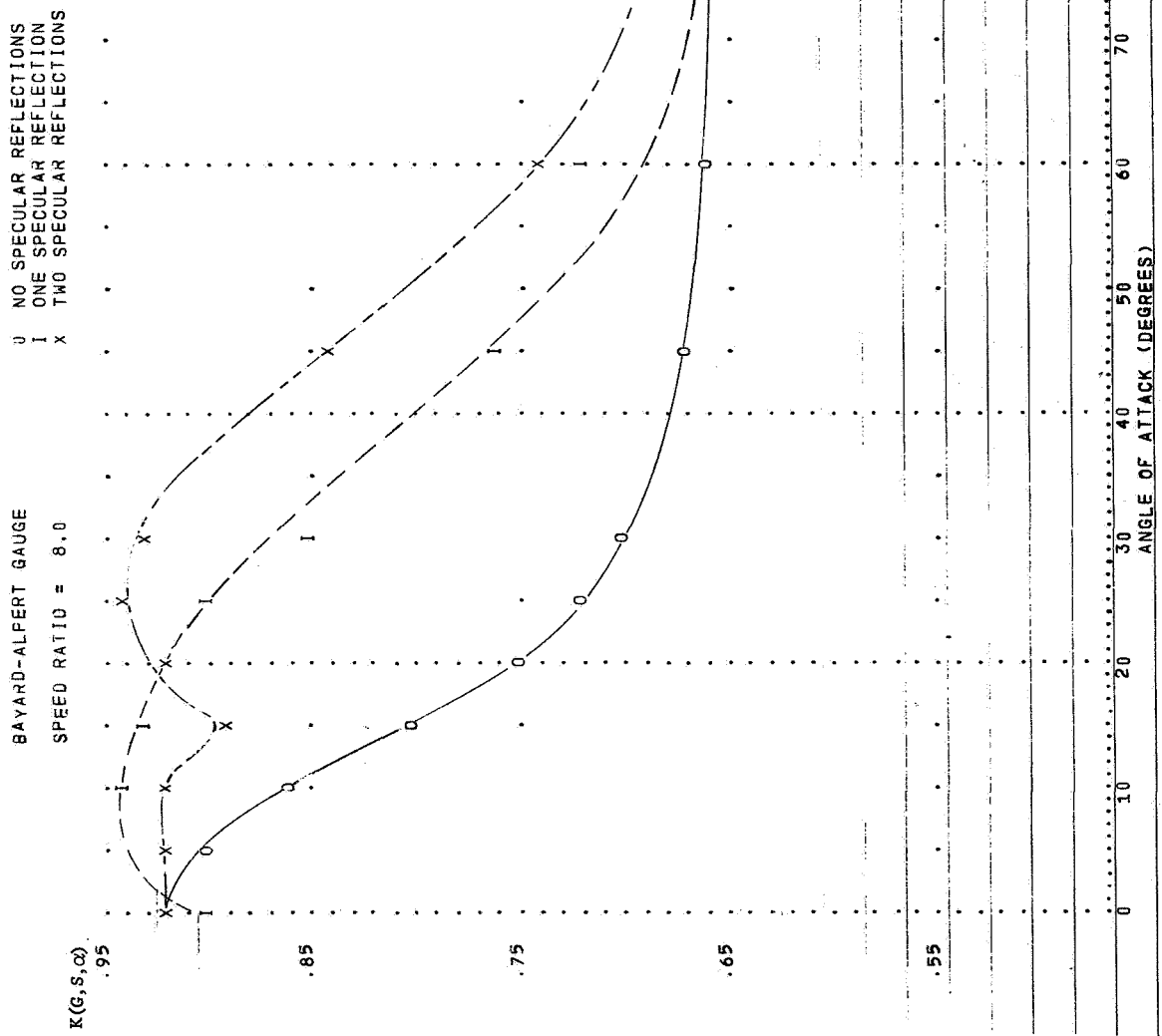


FIGURE 22

TRANSMISSION PROBABILITIES FOR THE VACUUM
GAUGES ON THE EXPLORER XVII AND EXPLORER XXXII
AERONAUTICS SATELLITES

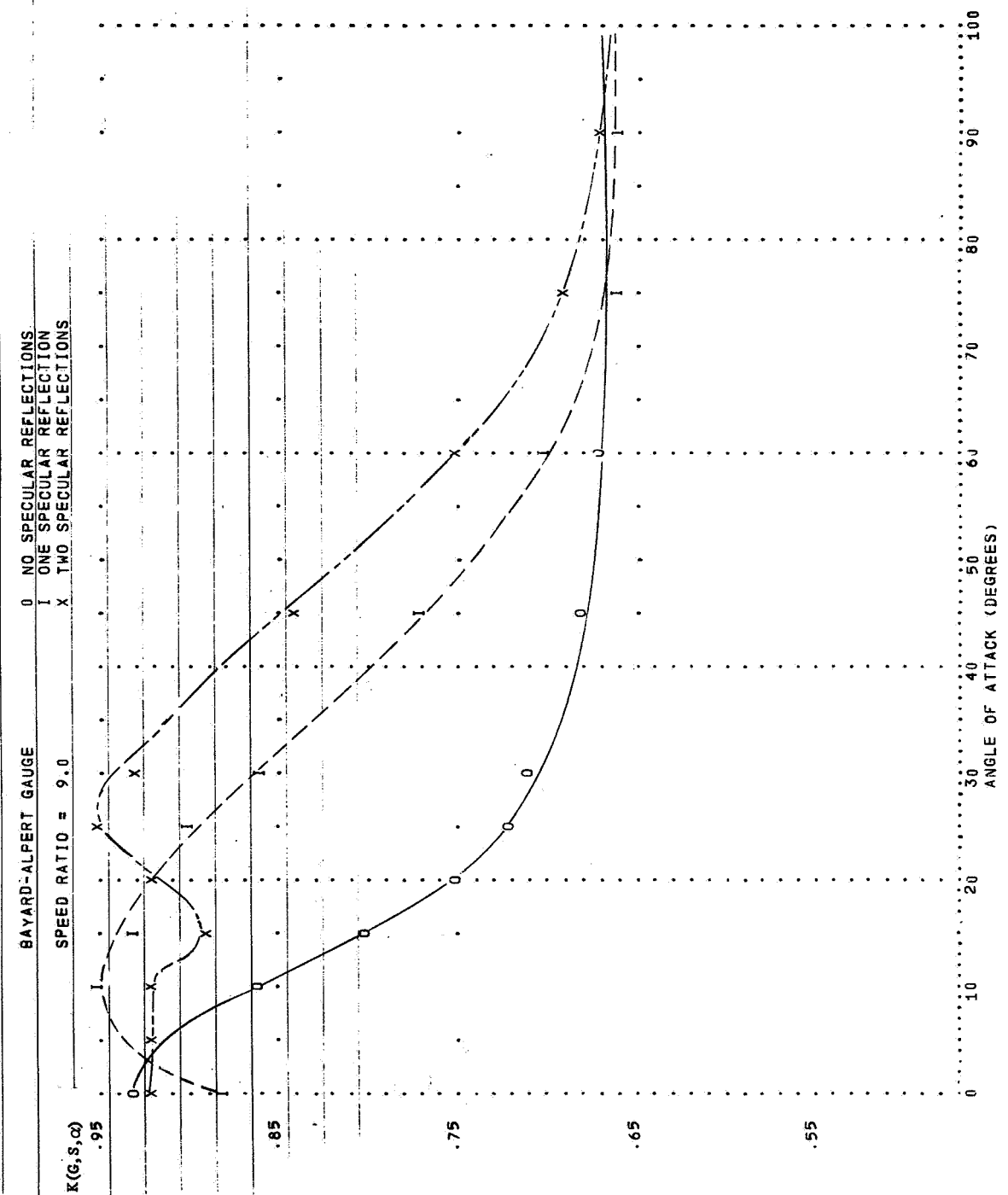


FIGURE 23

THEORETICAL PRESSURE RATIO RESPONSE FOR
THE VACUUM GAUGES ON THE EXPLORER XVI
AND EXPLORER XXXII AERONOMY SATELLITES

BAYARD-ALPERT GAUGE
SPEED RATIO = 2.0

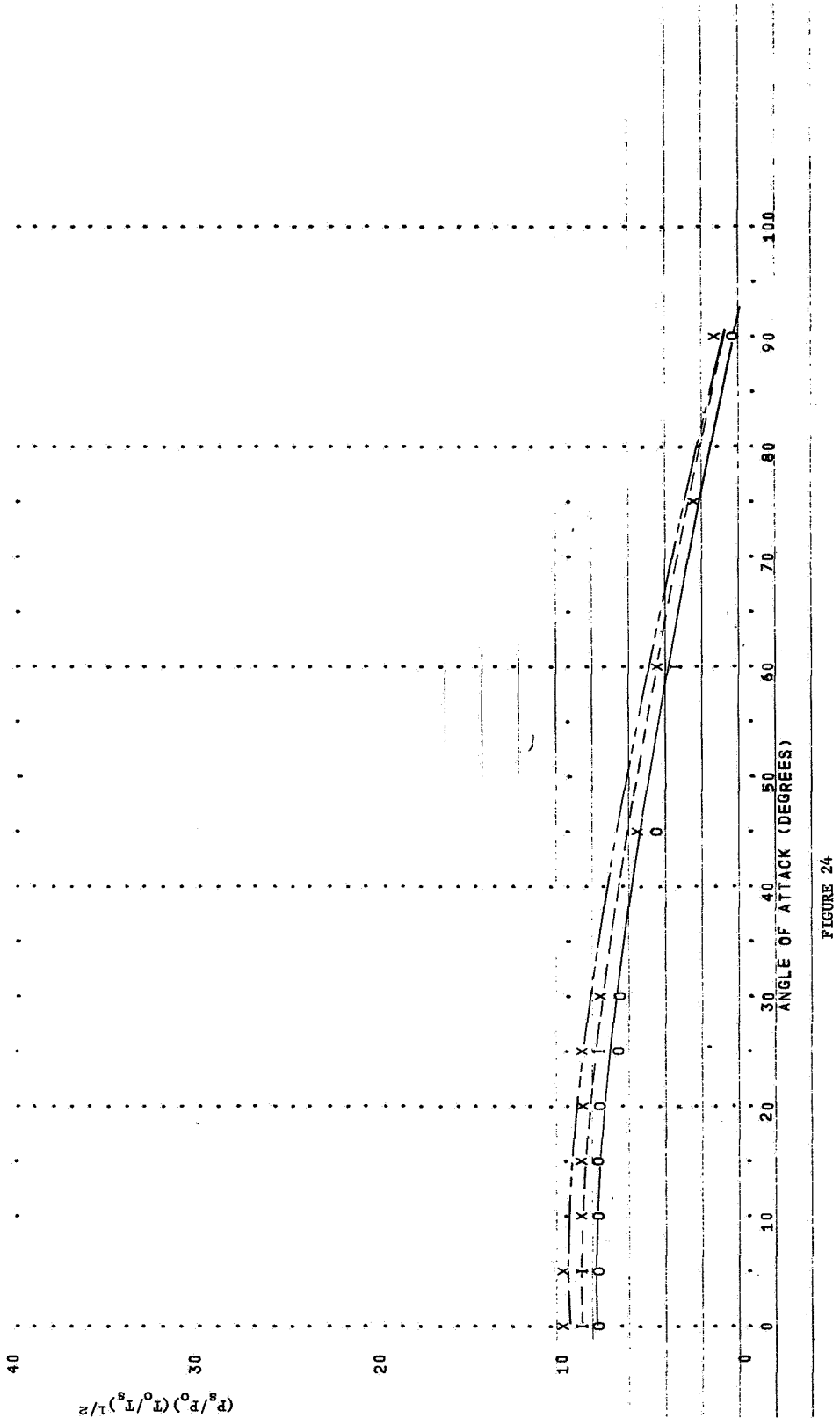


FIGURE 24

THEORETICAL PRESSURE RATIO RESPONSE FOR
THE VACUUM GAUGES ON THE EXPLORER XVII
AND EXPLORER XXXII AERONAUTICS SATELLITES

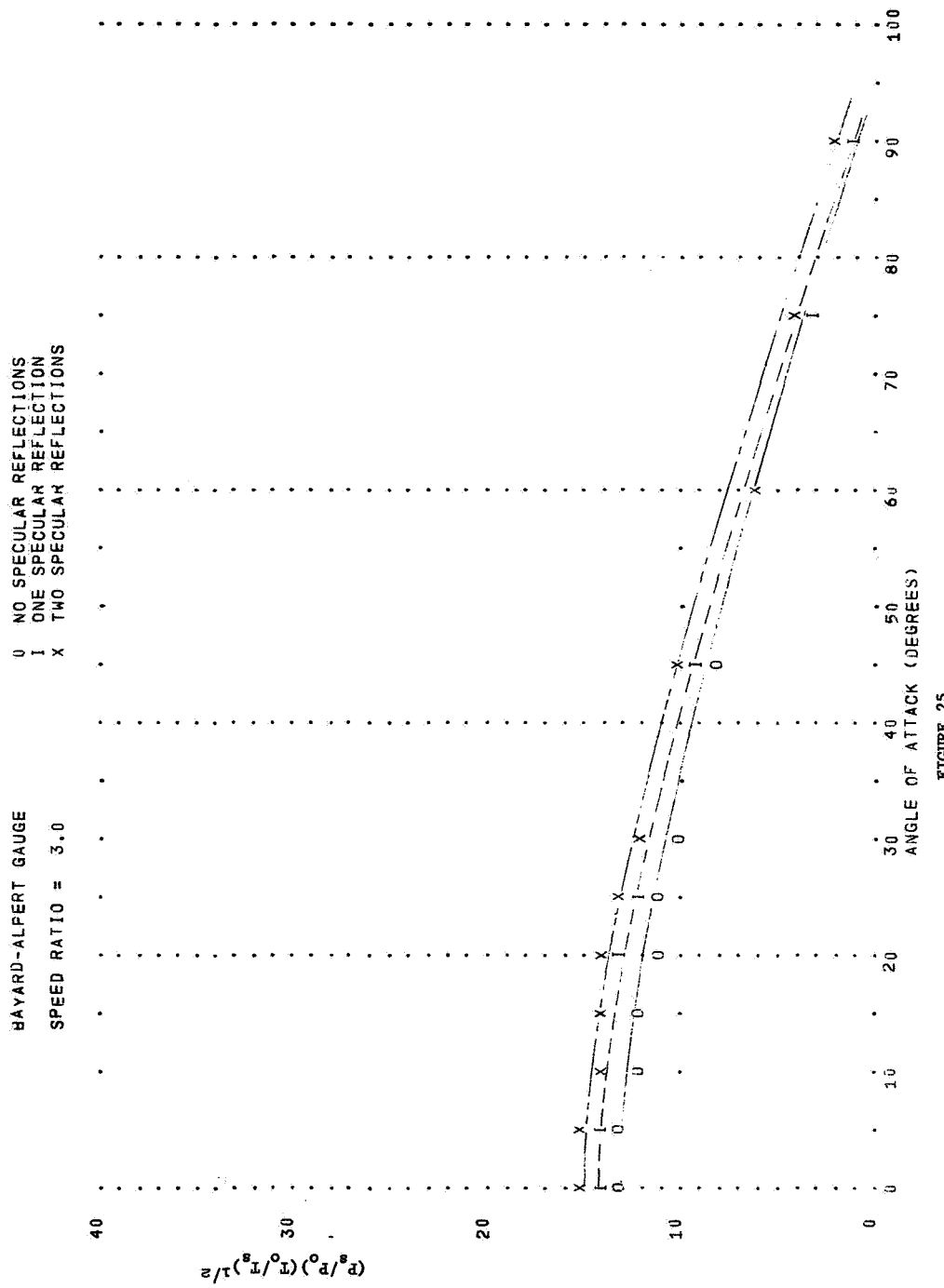


FIGURE 25

THE CRITICAL PRESSURE RATIO RESPONSE FOR
THE VACUUM GAUGES ON THE EXPLORER XVII
AND EXPLORER XXXII AERONAUTICS SATELLITES

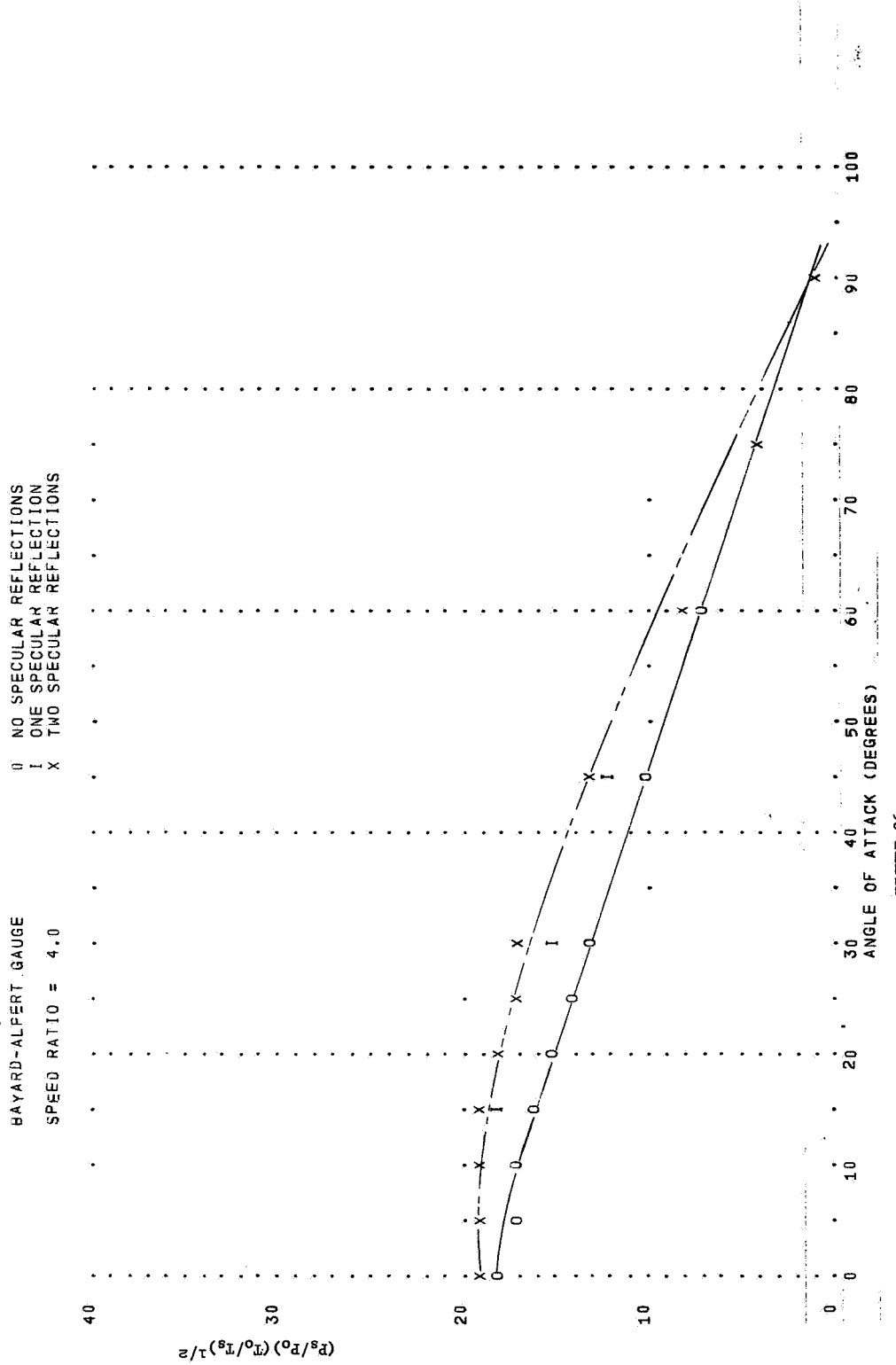


FIGURE 26

THEORETICAL PRESSURE RATIO RESPONSE FOR
THE VACUUM GAUGES ON THE EXPLORER XVII
AND EXPLORER XXXII AERODYNAMIC SATELLITES

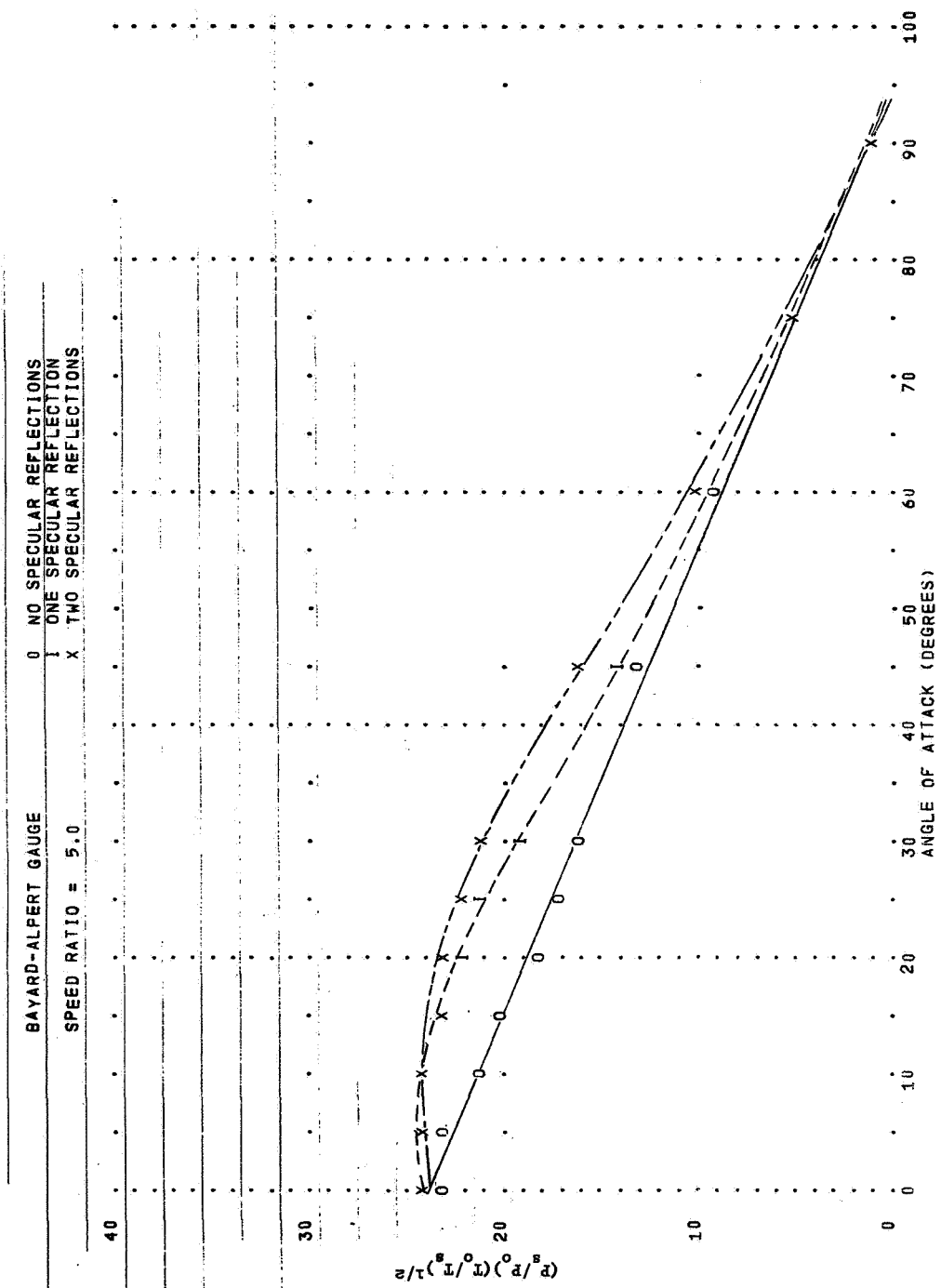


FIGURE 27

THEORETICAL PRESSURE RATIO RESPONSE FOR
THE VACUUM GAUGES ON THE EXPLORER XVI
AND EXPLORER XXXII AERONAUTICS SATELLITES

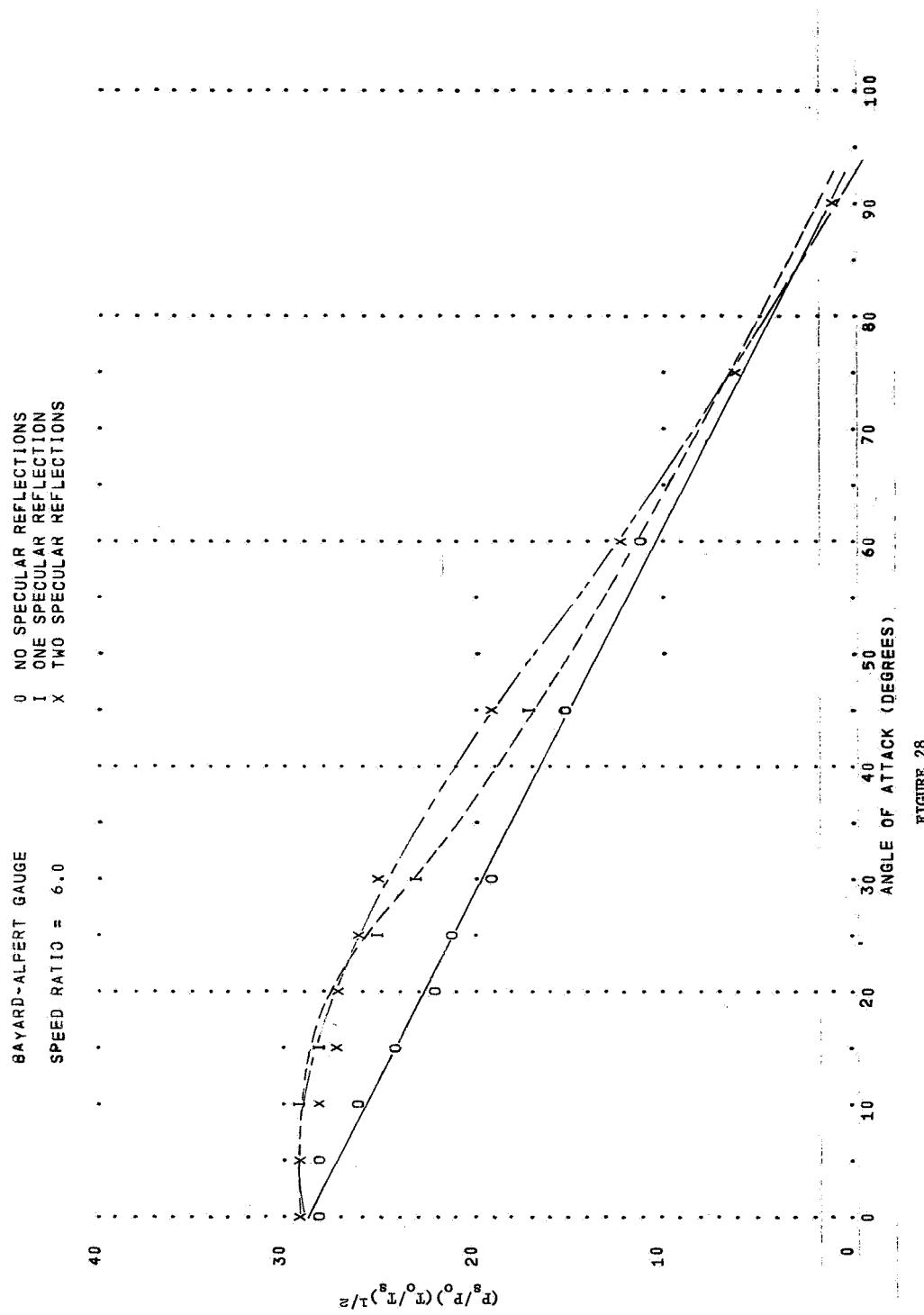


FIGURE 28

THEORETICAL PRESSURE RATIO RESPONSE FOR
THE VACUUM GAUGES ON THE EXPLORER XVII
AND EXPLORER XXXII AERONAUTICSATELLITES

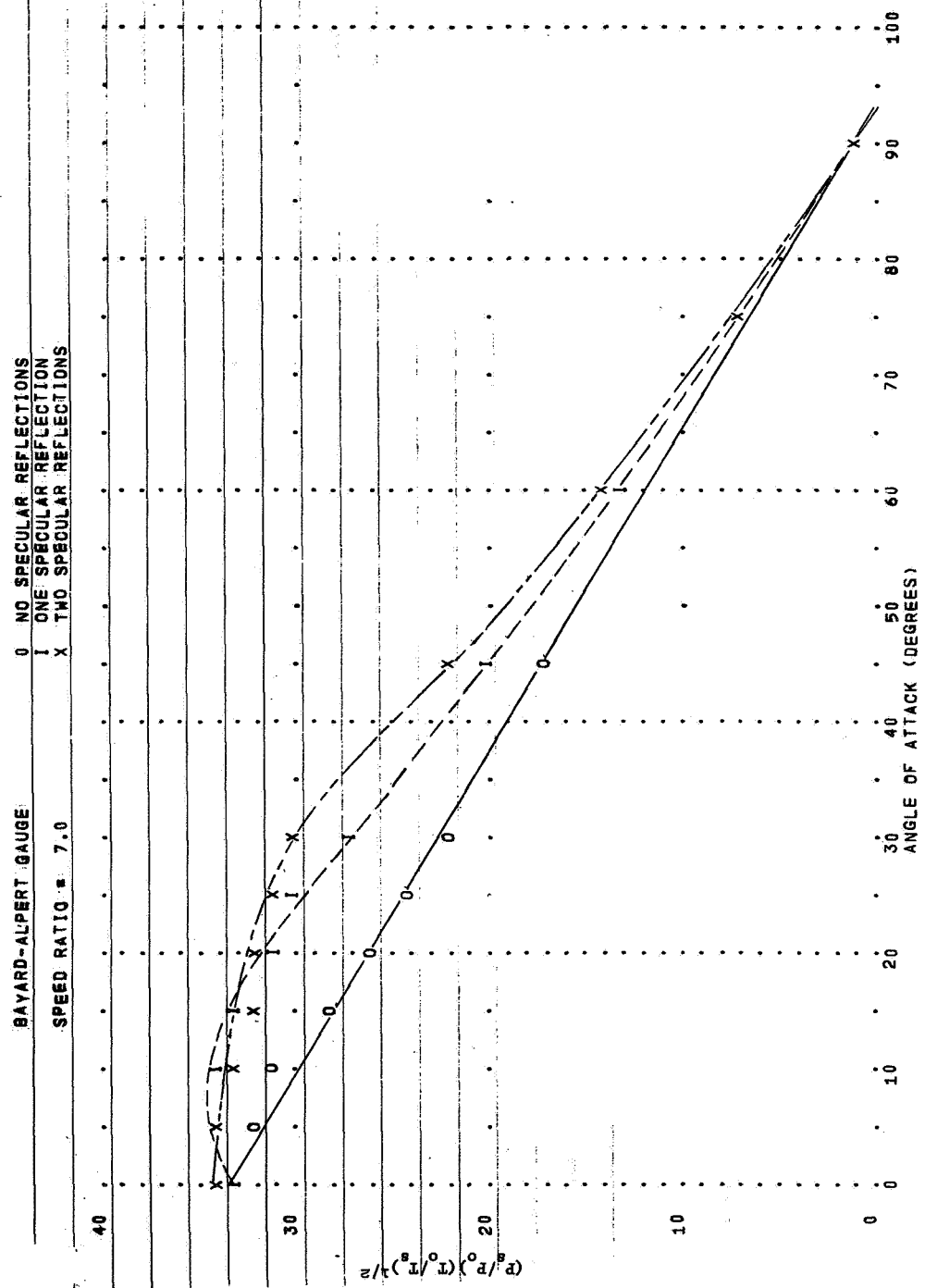


FIGURE 29

THEORETICAL PRESSURE RATIO RESPONSE FOR
THE VACUUM GAUGES ON THE EXPLORER XVII
AND EXPLORER XXXII AERONOMY SATELLITES

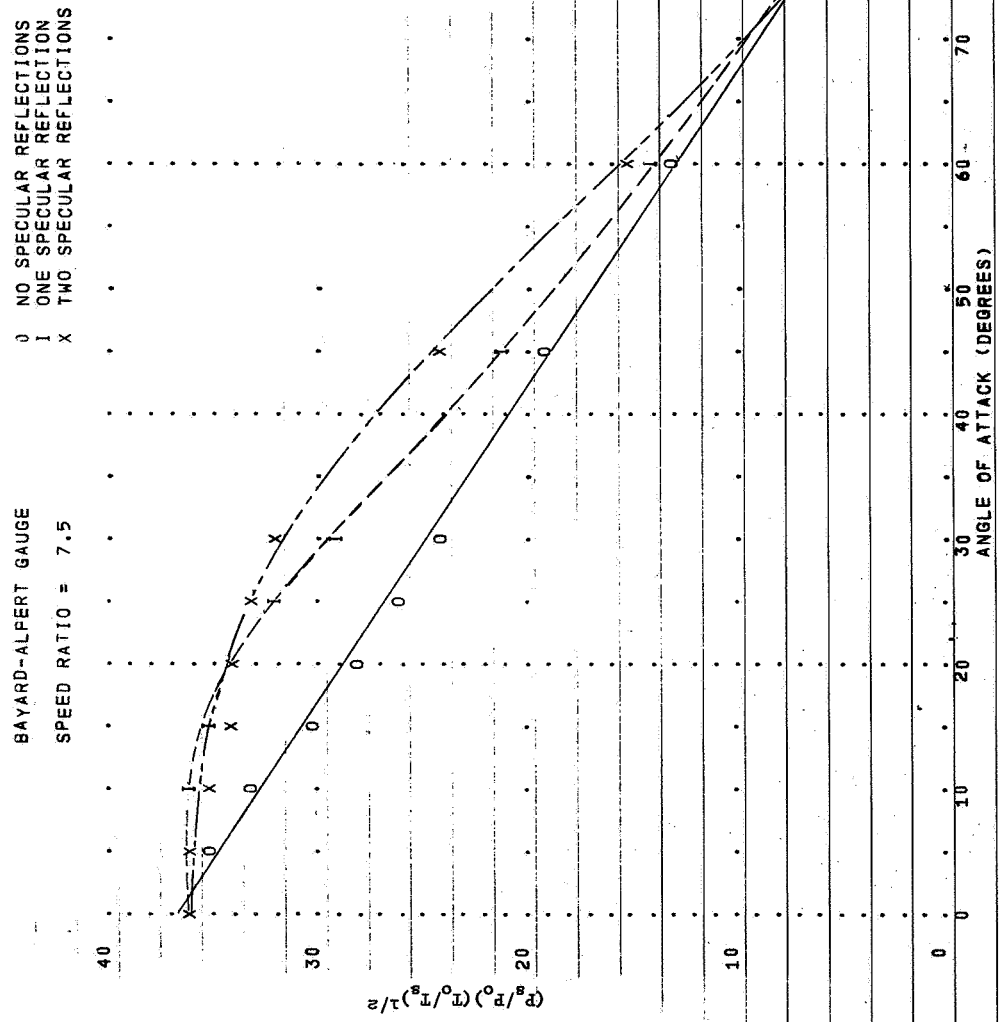


FIGURE 30

THEORITICAL PRESSURE RATIO RESPONSE FOR
THE VACUUM GAUGES ON THE EXPLORER XVII
AND EXPLORER XXXII AERONOMY SATELLITES

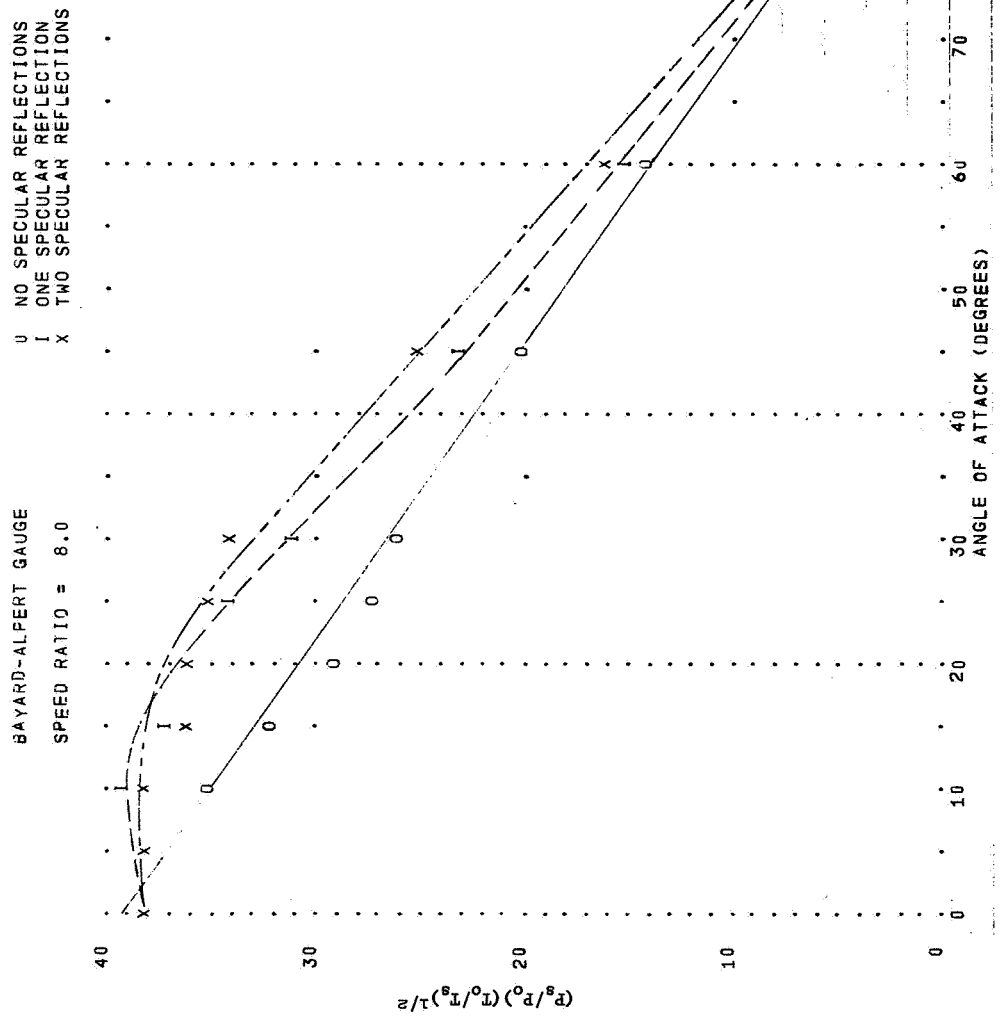


FIGURE 31

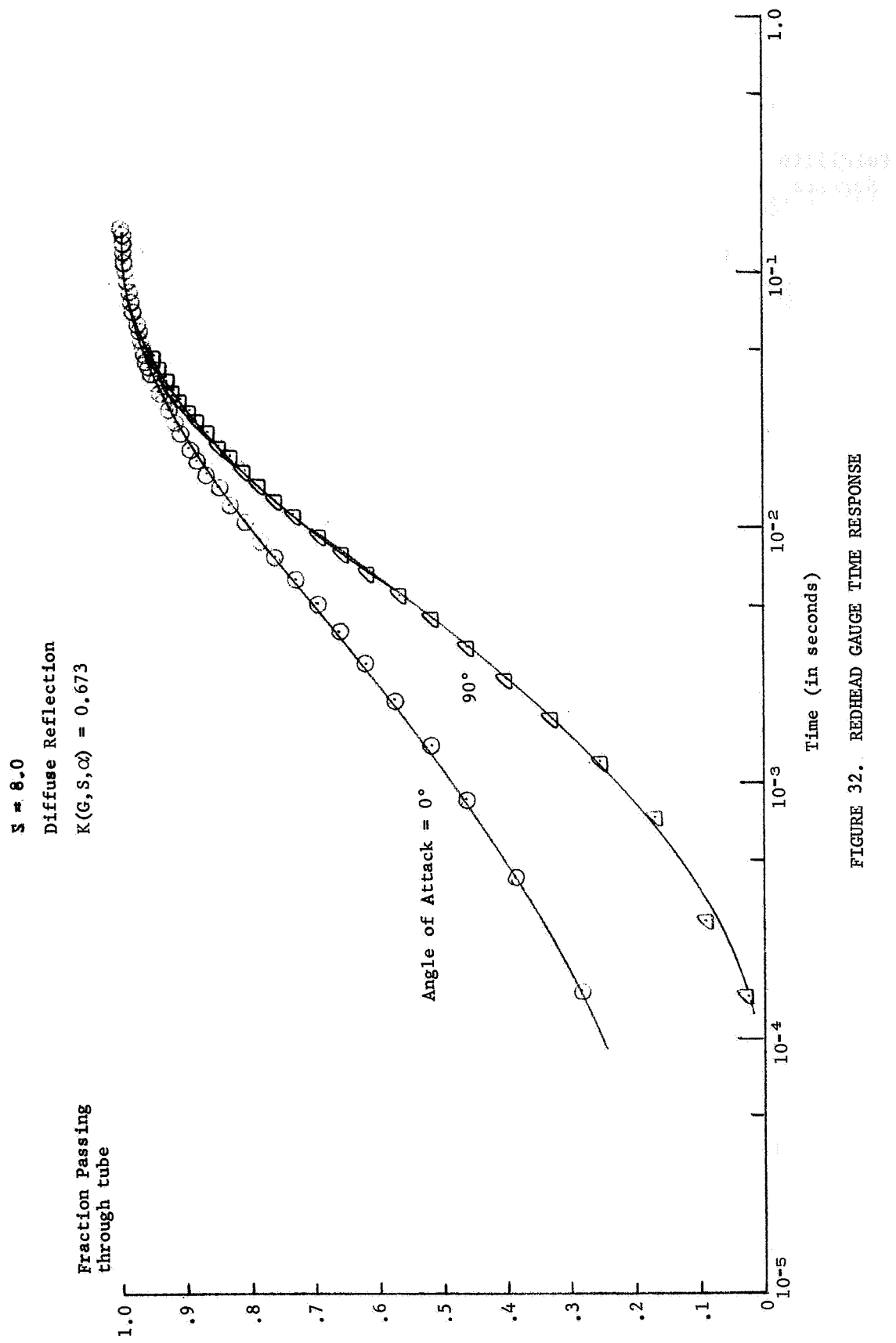


FIGURE 32. REDHEAD GAUGE TIME RESPONSE

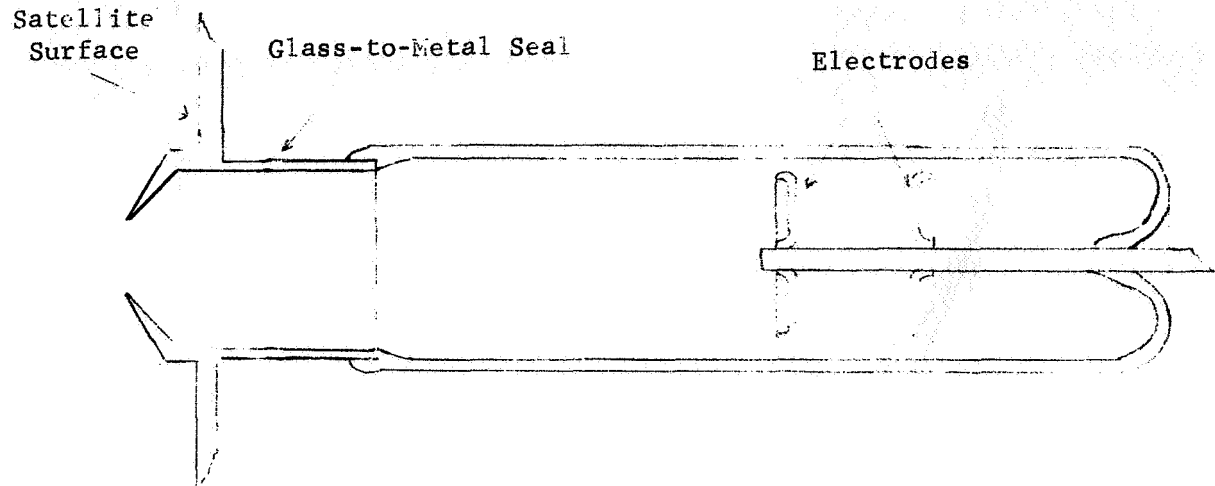


Figure 33a. Sketch of the Modified Redhead Gauge Configuration

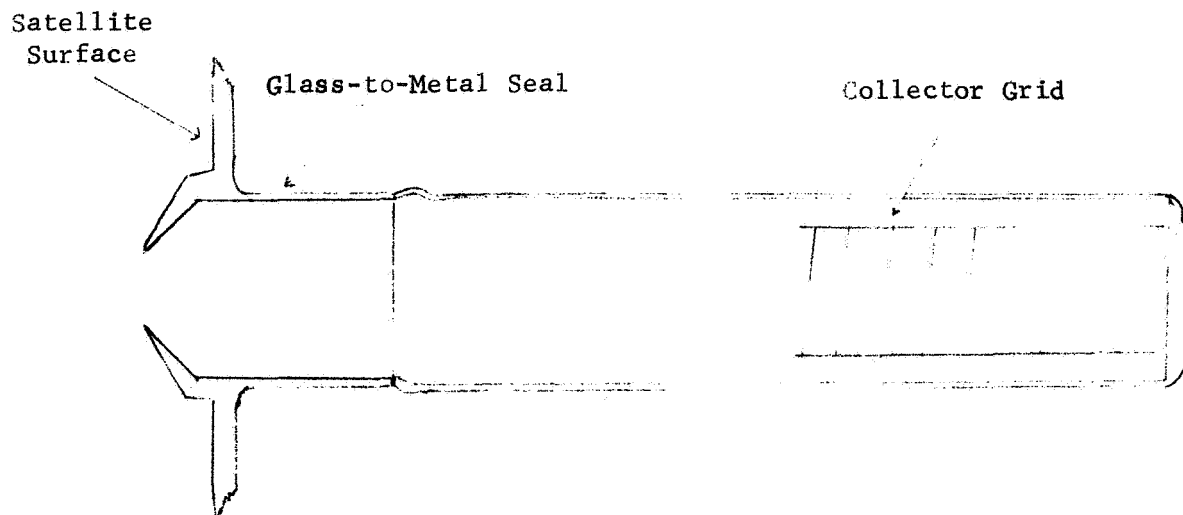


Figure 33b. Sketch of the Bayard-Alpert Gauge Configuration

REFERENCES

1. Horowitz, R., "S-6, An Aeronomy Satellite," *Advances in the Astronautical Sciences*, Vol. 12, 1963, pp. 21-39.
2. Newton, G. P., A. Horowitz, and W. Priester, "Atmospheric Densities from Explorer 17 Density Gages and a Comparison with Satellite Drag Data," *J. Geophys. Res.* 69, 4690-4692, 1962.
3. Spencer, N. W., G. P. Newton, C. A. Reber, L. H. Brace, and R. Horowitz, "New Knowledge of the Earth's Atmosphere from the Aeronomy Satellite (Explorer 17)," Goddard Space Flight Center Report X-651-64-114, 1964.
4. Newton, G. P., R. Horowitz, and W. Priester, "Atmospheric Density and Temperature Variations from the Explorer XVII Satellite and a Further Comparison with Satellite Drag," *Planet. Space Sci.*, 1965, Vol. 13, pp. 599-616.
5. Newton, G. P., D. T. Pelz, and G. E. Miller, "Response of Modified Redhead Magnetron and Bayard-Alpert Vacuum Gauges Aboard Explorer XVII," NASA TN D-2146, February 1964.
6. Newton, G., P. Silverman, and D. Pelz, "Interactions Between a Hypersonic Neutral Gas Beam and an Orificed Pressure Gauge Mounted in a Spinning Satellite," Goddard Space Flight Center Report X-621-68-396.
7. Newton, George P., David J. Pelz, and Hans Volland, "Direct In Situ Measurements of Wave Propagation in the Neutral Atmosphere," *Journal of Geophysical Research*, Vol. 74, No. 1, January 1969, pp. 183-196.
8. Pelz, D. and G. Newton, "Pressure Conversion Constants for Magnetron Ionization Gauges," *J. Vac. Sci. Tech.*, 4, 239, September-October 1967.

PAGE 56 LEFT BLANK

APPENDIX

Response of A Probe in Free Molecule Flow

The response of a probe in free molecule flow is easily shown in the following manner. Consider a cylindrical tube with an orifice (area A_o) at one end opening to the atmosphere and another orifice (area A_i) at the other end, opening to a sensor volume. The number of molecules which enter the orifice (A_o), which pass through the tube, and which exit the tube at the other orifice (A_i) is given by

$$Z_{in} = \frac{N_o \bar{V}_o}{4} F(S) A_o K_o(G, S, \alpha),$$

where

Z_{in} = number of molecules entering the sensor volume

N_o = number density of the ambient gas

\bar{V}_o = average speed of the ambient gas molecule

$$= \sqrt{\frac{8kT_o}{\pi m}}$$

k = Boltzmann's constant

m = mass of a molecule

T_o = temperature of the ambient gas

$$F(S) = e^{-S^2} + \sqrt{\pi} S [1 + ERF(S)]$$

S = speed ratio = $U \cos \alpha / V_m$

U = mass velocity of the probe relative to the gas

V_m = most probable speed of ambient molecules

α = angle between the normal to the orifice and the velocity vector

$K_o(G, S, \alpha)$ = Clausing probability factor in the direction from A_o to A_i

G = dummy variable to indicate geometry effects.

The number of molecules in the sensor volume which leave that volume through the orifice (A_i) and return to the atmosphere is given by

$$Z_{\text{out}} = \frac{N_s \bar{V}_s}{4} A_i K_i(G, 0, 0),$$

where

Z_{out} = number of molecules leaving the sensor volume

N_s = number density of the gas in the sensor volume

\bar{V}_s = average speed of the molecule in the sensor volume

$$= \sqrt{\frac{8kT_s}{\pi M}}$$

T_s = temperature of the gas in the sensor volume

$K_i(G, 0, 0)$ = Clausing probability function for the direction from A_i through A_o .

For equilibrium conditions,

$$Z_{\text{in}} = Z_{\text{out}}.$$

Thus,

$$\frac{N_o \bar{V}_o}{4} F(S) A_o K_o(G, S, \alpha) = \frac{N_s \bar{V}_s}{4} A_i K_i(G, 0, 0).$$

When $S = 0$, $T_o = T_s$ and $N_o = N_s$,

$$A_o K_o(G, 0, 0) = A_i K_i(G, 0, 0),$$

so that

$$K_i = \frac{A_o}{A_i} K_o(G, 0, 0).$$

Thus,

$$N_s = \frac{N_o \bar{V}_o F(S) K_o(G, S, \alpha) A_o}{\bar{V}_s K_o(G, 0, 0) \frac{A_o}{A_i} A_i}$$

$$= \frac{N_o \bar{V}_o F(S) K_o(G, S, \alpha)}{\bar{V}_s K_o(G, 0, 0)}$$

and

$$\frac{\bar{V}_o}{\bar{V}_s} = \sqrt{T_o/T_s},$$

so that

$$N_s = N_o \sqrt{T_o/T_s} F(S) \frac{K_o(G, S, \alpha)}{K_o(G, 0, 0)},$$

or, in terms of pressure, since $N_j = P_j/kT_j$,

$$\frac{P_s}{kT_s} = \frac{P_o}{kT_o} \sqrt{T_o/T_s} F(S) \frac{K_o(G, S, \alpha)}{K_o(G, 0, 0)}$$

$$P_s = P_o \sqrt{T_s/T_o} F(S) \frac{K_o(G, S, \alpha)}{K_o(G, 0, 0)}.$$

APPROVAL

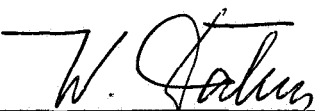
NASA TM X-53838

THE MOLECULAR KINETICS OF THE BAYARD-ALPERT AND
MODIFIED REDHEAD VACUUM GAUGES USED ON
EXPLORER XVII AND EXPLORER XXXII

by James O. Ballance

The information in this report has been reviewed for security classification. Review of any information concerning Department of Defense or Atomic Energy Commission programs has been made by the MSFC Security Classification Officer. This report, in its entirety, has been determined to be unclassified.

This document has also been reviewed and approved for technical accuracy.



W. K. Dahm
Chief, Aerophysics Division



E. D. Geissler
Director, Aero-Astroynamics Laboratory

DISTRIBUTION

DIR	<u>EXTERNAL</u>
S&E-DIR	Tech. & Sic. Info. Facility (25) Box 33
MS-IL (8)	College Park, Md. NASA Rep. (S-AK/RKT)
MS-IP	Langley Research Center Langley Sta. Hampton, Va.
DEP-T	Lewis Res. Center
CC-P	21000 Brookpark Cleveland, Ohio
MS-T (6)	Attn: Mr. L. Krause Mr. E. Richley Library
<u>S&E-ASTR</u> Mr. Moore	Goddard Space Flight Center Greenbelt, Md. Attn: Mr. G. Newton (10) Mr. N. W. Spencer (5) Library
<u>S&E-SSL</u> Mr. Heller Mr. Hembree	JPL 4800 Oak Grove Dr. Pasadena, Calif.
<u>S&E-AERO</u> Dr. Geissler Mr. Vaughan Mr. R. E. Smith Dr. Heybey Mr. J. Johnson Mr. J. Carter Mr. Baker Mr. Dahm Mr. Ballance (40) Mr. Horn Mr. Lindberg Mr. Lovingood Dr. DeVries Mr. D. Weidner Mr. G. Swenson	Ames Res. Center Moffett Field, Calif. Manned Spacecraft Center Houston, Texas Attn: Library Arthur D. Little, Inc. Cambridge, Mass. Northrop Space Labs. Huntsville, Ala.

EXTERNAL DISTRIBUTION (Continued)

AEDC Arnold Air Force Station, Tenn.	Atlantic Research Corp. Missile Systems Div. 3333 Harbor Blvd. Costa Mesa, Calif 92626
ARO, Inc. AEDC Arnold Air Force Station, Tenn. Attn: Library	Attn: Library Dr. R. Chuan Mr. D. Wallace
Univ. of Ill. Urbana, Ill. Attn: Library Dr. Yen Dr. G. Karr	Univ. of Calif. Radiation Laboratory Livermore, Calif. Attn: Library Dr. Hurlbut
Mass. Inst. of Tech. Cambridge, Mass. Attn: Dr. R. Stickney Dr. L. Trilling Library	Lockheed Aircraft Corp. Huntsville, Ala. Attn: Dr. C. Fan Mr. J. Robertson Mr. H. Shirley Library
Univ. of Ala. University, Ala. Attn: Dr. W. Schaetzle Library	Brown Engineering Co. Huntsville, Alabama Attn: R. Watson Library
Ga. Inst. of Tech. Atlanta, Ga. Attn: Dr. A. B. Huang Library	Heat Technology Lab. Huntsville, Ala.
Inst. of Aerophysics Univ. of Toronto Toronto, Canada Attn: P. C. Hughes Dr. G. N. Patterson Library	Univ. of Mich. Ann Arbor, Michigan Attn: George Carignan Hasso Niemann David Taeusch Library
Cornell Aeronautical Lab., Inc. Buffalo, New York	<u>NASA Hdqs.</u> OSSA - R. Horowitz - Dr. Fellows - Mr. Dubin
McDonnell Aircraft Corp. P. O. Box 516 Attn: E. S. J. Wange St. Louis, Missouri	OART - Mr. Schwartz